



University of Kentucky  
UKnowledge

---

Theses and Dissertations--Biomedical  
Engineering

Biomedical Engineering

---

2014

## HUMAN CARDIOVASCULAR RESPONSES TO ARTIFICIAL GRAVITY VARIABLES: GROUND-BASED EXPERIMENTATION FOR SPACEFLIGHT IMPLEMENTATION

Mark Howarth

University of Kentucky, [mark.howarth@uky.edu](mailto:mark.howarth@uky.edu)

[Right click to open a feedback form in a new tab to let us know how this document benefits you.](#)

---

### Recommended Citation

Howarth, Mark, "HUMAN CARDIOVASCULAR RESPONSES TO ARTIFICIAL GRAVITY VARIABLES: GROUND-BASED EXPERIMENTATION FOR SPACEFLIGHT IMPLEMENTATION" (2014). *Theses and Dissertations--Biomedical Engineering*. 14.

[https://uknowledge.uky.edu/cbme\\_etds/14](https://uknowledge.uky.edu/cbme_etds/14)

This Doctoral Dissertation is brought to you for free and open access by the Biomedical Engineering at UKnowledge. It has been accepted for inclusion in Theses and Dissertations--Biomedical Engineering by an authorized administrator of UKnowledge. For more information, please contact [UKnowledge@lsv.uky.edu](mailto:UKnowledge@lsv.uky.edu).

## STUDENT AGREEMENT:

I represent that my thesis or dissertation and abstract are my original work. Proper attribution has been given to all outside sources. I understand that I am solely responsible for obtaining any needed copyright permissions. I have obtained needed written permission statement(s) from the owner(s) of each third-party copyrighted matter to be included in my work, allowing electronic distribution (if such use is not permitted by the fair use doctrine) which will be submitted to UKnowledge as Additional File.

I hereby grant to The University of Kentucky and its agents the irrevocable, non-exclusive, and royalty-free license to archive and make accessible my work in whole or in part in all forms of media, now or hereafter known. I agree that the document mentioned above may be made available immediately for worldwide access unless an embargo applies.

I retain all other ownership rights to the copyright of my work. I also retain the right to use in future works (such as articles or books) all or part of my work. I understand that I am free to register the copyright to my work.

## REVIEW, APPROVAL AND ACCEPTANCE

The document mentioned above has been reviewed and accepted by the student's advisor, on behalf of the advisory committee, and by the Director of Graduate Studies (DGS), on behalf of the program; we verify that this is the final, approved version of the student's thesis including all changes required by the advisory committee. The undersigned agree to abide by the statements above.

Mark Howarth, Student

Dr. Abhijit Patwardhan, Major Professor

Dr. Abhijit Patwardhan, Director of Graduate Studies

HUMAN CARDIOVASCULAR RESPONSES TO  
ARTIFICIAL GRAVITY VARIABLES:  
GROUND-BASED EXPERIMENTATION FOR  
SPACEFLIGHT IMPLEMENTATION

---

DISSERTATION

---

A dissertation submitted in partial fulfillment of the  
requirements for the degree of Doctor of Philosophy in the  
College of Engineering  
at the University of Kentucky

By  
Mark Steven Howarth

Lexington, Kentucky

Director: Dr. Abhijit R. Patwardhan, Professor of Biomedical Engineering

Lexington, Kentucky

2014

Copyright © Mark Steven Howarth 2014

## ABSTRACT OF DISSERTATION

### HUMAN CARDIOVASCULAR RESPONSES TO ARTIFICIAL GRAVITY VARIABLES: GROUND-BASED EXPERIMENTATION FOR SPACEFLIGHT IMPLEMENTATION

One countermeasure to cardiovascular spaceflight deconditioning being tested is the application of intermittent artificial gravity provided by centripetal acceleration of a human via centrifuge. However, artificial gravity protocols have not been optimized for the cardiovascular system, or any other physiological system for that matter. Before artificial gravity protocols can be optimized for the cardiovascular system, cardiovascular responses to the variables of artificial gravity need to be quantified.

The research presented in this document is intended to determine how the artificial gravity variables, radius (gravity gradient) and lower limb exercise, affect cardiovascular responses during centrifugation. Net fluid (blood) shifts between body segments (thorax, abdomen, upper leg, lower leg) will be analyzed to assess the cardiovascular responses to these variables of artificial gravity, as well as to begin to understand potential mechanism(s) underlying the beneficial orthostatic tolerance response resulting from artificial gravity training.

Methods: Twelve healthy males experienced the following centrifuge protocols. Protocol A: After 10 minutes of supine control, the subjects were exposed to rotational  $1 G_z$  at radius of rotation 8.36 ft (2.54 m) for 2 minutes followed by 20 minutes alternating between 1 and 1.25  $G_z$ . Protocol B: Same as A, but lower limb exercise (70%  $V_{O2max}$ ) preceded ramps to 1.25  $G_z$ . Protocol C: Same as A but radius of rotation 27.36 ft (8.33 m).

Results: While long radius without exercise presented an increased challenge for the cardiovascular system compared to short radius without exercise, it is likely at the expense of more blood “pooling” in the abdominal region. Whereas short radius with exercise provided a significant response compared to short radius without exercise. More fluid loss occurred from the

thorax and with the increased fluid loss from the thorax blood did not “pool” in the abdominal region but instead was essentially “mobilized” to the upper and lower leg. The exercise fluid shift profile presented in this document is applicable to not only artificial gravity protocol design but also proposes a mechanistic reason as to why certain artificial gravity protocols are more effective than others in increasing orthostatic tolerance.

KEYWORDS: Artificial Gravity, Spaceflight Countermeasures, Centrifugation, Cardiovascular Regulation, Electrical Impedance Plethysmography

Multimedia Elements Used: JPEG (.jpg)

Mark Steven Howarth

February 28, 2014

HUMAN CARDIOVASCULAR RESPONSES TO  
ARTIFICIAL GRAVITY VARIABLES:  
GROUND-BASED EXPERIMENTATION FOR  
SPACEFLIGHT IMPLEMENTATION

By

Mark Steven Howarth

Dr. Abhijit R. Patwardhan  
Director of Dissertation

Dr. Abhijit R. Patwardhan  
Director of Graduate Studies

February 28, 2014

## Freedom Is Not Free



I would like to dedicate this work to those that have died in battle fighting to keep America free from terrorism. Those that volunteer their lives to protect the principles on which America was founded allow the rest of us in society to carry on our daily lives with relative ease. I was fortunate enough to remain stateside with cushy luxuries while many (including friends and family) deployed to “the suck”. It is my hope that this work will benefit society, particularly the space program, at some point in the future. Otherwise, I have published a book that will simply collect dust on a library shelf, or occupy digital space on some hard drive. If that is the case, then perhaps I should have just joined my friends and family in “the suck”. It remains to be seen if this book is the ticket for admission to a happy, successful, and meaningful career.

## ACKNOWLEDGMENTS

First and foremost I would like to thank Dr. David Randall. Without him, it is unlikely that I would have been able to navigate the political waters of a dissertation committee. I would also like to thank Dr. Brian Jackson for our informal discussions at the gym. I would like to thank my committee members: Dr. Charles Knapp, Dr. Abhijit Patwardhan, Dr. Ken Campbell, and Joyce Evans for their knowledge, guidance, and editorial suggestions. We had some heated discussions that often left me puzzled. Post-meeting discussions with Dr. Randall allowed me to keep an even keel and keep plowing forward. I would also like to thank the outsider reviewer, Dr. Kevin Donohue, for his time.

I would like to thank all of the staff members at NASA Ames Research Center that allowed this study to be possible, particularly Dr. Fritz Moore, Dr. Ralph Pelligra, Rick Ryzinga, and Russ Westbrook. I would also like to thank all of our test subjects, although, most all of them had a blast riding the centrifuge and being instrumented to the hilt. Thanks also belong to the taxpayer whose money supports NASA and also supported the NASA EPSCoR grants that helped fund this study.

Dr. Mike Stenger left the University of Kentucky within a couple years of my arrival to go work at NASA. He first introduced me to MATLAB and SAS programming which gave me enough basic knowledge to pick up the rest along the way in order to complete my data analysis. Helena Truszczynska is to thank for helping me develop the exact SAS code I wanted. It would have been fun to have Mike around longer for research purposes, and as a gym partner. He was and probably still is a BAMF.

I would also like to thank my friends and family that have been there at the various stages of this process. I suppose we deal with the stress and rigors of academic pursuit in different ways. My vices were my hair and the gym. I have had curly hair like Tom Jones, blonde hair like Hulk Hogan and Brad Pitt, buzz cut hair, and more recently long hair like Fabio and Troy Polamalu. Thank you for the Johnson Center at UK. I have had many a workout in there either pushing



weights or running circles around the track blowing off stress or constructively vetting out ideas. To match the hair changes, I have weighed at times anywhere from the 170's to 248 pounds, depending on if it was "bulking season" or not.

Finally, I would also like to thank my undergraduate mentor Dr. John Watret. We had a conversation mid-way through this process and he reminded me of the importance of actually completing the dissertation so that I was not another statistic of being Ph.D. A.B.D. (all but dissertation). I have never been a quitter, I started the Ph.D. process and by God I actually finished! That puts me with company the likes of less than 3% of the U.S. population, and less than 1% of the world population.

## TABLE OF CONTENTS

Acknowledgments .....	iii
List of Tables .....	viii
List of Figures .....	ix
Chapter One: Introduction .....	1
Scientific Problem .....	4
Original Scientific Contribution .....	5
Chapter Two: Background .....	6
Microgravity and Artificial Gravity .....	6
Artificial Gravity via Centrifugation .....	9
Physics of Artificial Gravity via Centrifugation .....	12
Ground-Based Artificial Gravity via Centrifugation .....	14
Chapter Three: Specific Aims .....	15
Rationale .....	15
Chapter Four: Experiment Methodology .....	18
Experimental Protocol Design Background .....	18
Experimental Protocols .....	20
Evaluation of Experimental Protocols .....	23
Chapter Five: Data Analysis .....	27
Subjects .....	27
Instrumentation .....	27
Data Acquisition .....	29

Mean Values .....	30
Statistics .....	30
Data Selection .....	32
Chapter Six: Feasibility of Electrical Impedance Plethysmography	
Measurement.....	35
Chapter Seven: Results.....	
Specific Aim 1 .....	49
Specific Aim 2 .....	57
Specific Aim 3 .....	65
Specific Aim 4 .....	68
Chapter Eight: Discussion .....	
Specific Aim 1 .....	70
Thorax.....	70
Abdomen .....	70
Upper Leg .....	71
Lower Leg .....	72
Summary .....	72
Specific Aim 2 .....	74
Thorax.....	74
Abdomen .....	75
Upper Leg .....	75
Lower Leg .....	76
Summary .....	77
Specific Aim 3 .....	78
Specific Aim 4 .....	79

Chapter Nine: Noteworthy Findings .....	80
Simultaneous Plethysmography Measurements .....	80
Artificial Gravity Protocol Design .....	80
Underlying Mechanism(s) Explaining Increased Orthostatic Tolerance ..	82
Chapter Ten: Study Limitations and Recommendations for Future Work .....	84
Supine Exercise Response .....	84
Upright Tilt Fluid Shift Profile of Subjects Pre- and Post-AG Training .....	84
Significance of Leg Position on Fluid Shift Profile .....	85
Appendices .....	86
Appendix A: Butterworth Low-Pass Filter MATLAB Code .....	86
Appendix B: Electrical Impedance Plethysmography .....	87
Background .....	87
Mathematical Expression for Volume of Electrical Conductors ...	88
Derivation of Impedance Volume Percent Change .....	90
References .....	91
Vita .....	96

## LIST OF TABLES

Table 4.1: Centrifuge radii, rotation rates, $G_z$ levels, and slopes of $G_z$ gradient..	23
Table 7.1: Thoracic fluid shifts SRC- (Protocol A) versus LRC- (Protocol C) statistical summary .....	50
Table 7.2: Abdominal fluid shifts SRC- (Protocol A) versus LRC- (Protocol C) statistical summary .....	52
Table 7.3: Upper leg fluid shifts SRC- (Protocol A) versus LRC- (Protocol C) statistical summary .....	54
Table 7.4: Lower leg fluid shifts SRC- (Protocol A) versus LRC- (Protocol C) statistical summary .....	56
Table 7.5: Thoracic fluid shifts SRC- (Protocol A) versus SRC+ (Protocol B) statistical summary .....	58
Table 7.6: Abdominal fluid shifts SRC- (Protocol A) versus SRC+ (Protocol B) statistical summary .....	60
Table 7.7: Upper leg fluid shifts SRC- (Protocol A) versus SRC+ (Protocol B) statistical summary .....	62
Table 7.8: Lower leg fluid shifts SRC- (Protocol A) versus SRC+ (Protocol B) statistical summary .....	64
Table 7.9: Heart rates SRC- (Protocol A) versus LRC- (Protocol C) statistical summary .....	67
Table 7.10: Heart rates SRC- (Protocol A) versus SRC+ (Protocol B) statistical summary .....	69

## LIST OF FIGURES

Figure 2.1: NASA Ames Human Powered Centrifuge .....	10
Figure 2.2: Cardinal axes of the human body .....	11
Figure 2.3: Centrifuge force vector diagram. Earth gravitational force ( $G_x$ ), centrifugal force ( $G_z$ ), net gravito-inertial force ( $G_{zx}$ ).....	14
Figure 4.1: NASA Ames 20G Centrifuge .....	19
Figure 4.2: Centrifuge protocols A, B, and C .....	21
Figure 4.3: Centrifuge radii and $G_z$ levels at head and foot .....	24
Figure 4.4: $G_z$ gradients from head to foot .....	25
Figure 4.5: Net gravito-inertial forces ( $G_{zx}$ ) at head and foot.....	26
Figure 5.1: Subject instrumentation .....	29
Figure 5.2: Fluid shift data segments (in red) and time point nomenclature for Protocols A, B, and C .....	33
Figure 5.3: Heart rate data segments (in red) and time point nomenclature for Protocols A, B, and C .....	34
Figure 6.1: Average thoracic fluid shifts for SRC-.....	36
Figure 6.2: Individual subject thoracic fluid shifts for SRC-.....	36
Figure 6.3: Average abdominal fluid shifts for SRC-.....	38
Figure 6.4: Individual subject abdominal fluid shifts for SRC-.....	38
Figure 6.5: Average upper leg fluid shifts for SRC- .....	40
Figure 6.6: Individual subject upper leg fluid shifts for SRC- .....	40
Figure 6.7: Average lower leg fluid shifts for SRC- .....	42
Figure 6.8: Individual subject lower leg fluid shifts for SRC- .....	42
Figure 6.9: Average thoracic fluid shifts for 70° tilt.....	45
Figure 6.10: Individual subject thoracic fluid shifts for 70° tilt .....	45
Figure 6.11: Average abdominal fluid shifts for 70° tilt.....	46
Figure 6.12: Individual subject abdominal fluid shifts for 70° tilt .....	46
Figure 6.13: Average upper leg fluid shifts for 70° tilt .....	47
Figure 6.14: Individual subject upper leg fluid shifts for 70° tilt .....	47

Figure 6.15: Average lower leg fluid shifts for 70° tilt.....	48
Figure 6.16: Individual subject lower leg fluid shifts for 70° tilt.....	48
Figure 7.1: Thoracic fluid shifts SRC- versus LRC- .....	49
Figure 7.2: Abdominal fluid shifts SRC- versus LRC- .....	51
Figure 7.3: Upper leg fluid shifts SRC- versus LRC- .....	53
Figure 7.4: Lower leg fluid shifts SRC- versus LRC- .....	55
Figure 7.5: Thoracic fluid shifts SRC- versus SRC+ .....	57
Figure 7.6: Abdominal fluid shifts SRC- versus SRC+ .....	59
Figure 7.7: Upper leg fluid shifts SRC- versus SRC+ .....	61
Figure 7.8: Lower leg fluid shifts SRC- versus SRC+ .....	63
Figure 7.9: Heart rates SRC- versus LRC- .....	66
Figure 7.10: Heart rates SRC- versus SRC+ .....	68

## Chapter One: Introduction

In order to realize human voyages of space exploration, we must develop both a new understanding of the risks posed by the potentially dangerous levels of radiation and extended weightlessness as well as a more effective means of coping with these risks (Buckey 1999, White and Averner 2001). These are issues that must be dealt with now, before fundamental decisions are reached concerning the appropriate time for humans to move away from Earth on voyages of exploration (White and Averner 2001).

Voyages of exploration will subject space travelers to three serious and related challenges: 1) changes in the physical forces on and within the body brought about by a reduction in weight of the body's components; 2) psychosocial changes induced by the long-term confinement of such a voyage without the possibility of escape; and 3) changes in the levels and types of radiation in the environment (White and Averner 2001, Paloski et al. 2009). These changes, which act simultaneously, precipitate a cascade of time-related events in the human body about which we have been learning slowly for the past 50 years (White and Averner 2001). The integrated responses of the body to these challenges present real risks to the health of the humans undertaking such missions and to the satisfactory completion of the missions themselves (White and Averner 2001). The challenges of physiological deconditioning, behavioral stresses, and radiation pose serious threats to humans aboard long-duration spaceflight missions (White and Averner 2001, Clement et al. 2007, Paloski et al. 2009). The principal physiological deconditioning risks are related to physical and functional deterioration of the musculo-skeletal systems, loss of regulation of the blood circulation, decreased aerobic capacity, and altered sensory-motor system performance (White and Averner 2001, Clement et al. 2007, Paloski et al. 2009). Artificial gravity has the potential to fully mitigate the risk of physiological



deconditioning by preventing the adaptive responses from occurring (Clement et al. 2007, Paloski et al. 2009).

Artificial gravity research over the past 50 years has made sporadic progress, owing to the ebb and flow of funding associated with perceived programmatic needs for robust countermeasures against the untoward aspects of physiological deconditioning of humans during planned spaceflight missions (Paloski et al. 2009). The United States' announcement of a Vision for Space Exploration involving long-duration flights to Mars, coupled with the current absence of effective countermeasures to offset the untoward physiological effects of long-term microgravity exposure, has drawn increased attention to artificial gravity (Paloski et al. 2009). The unknown, but predictable effects of one to three years exposure to hypogravity (0G during transit and 0.38G while on the Mars planetary surface) are not likely to be countered by combinations of exercise and pharmaceuticals (Clement et al. 2007, Paloski et al. 2009).

To succeed in the goal of a human mission to Mars, the human risks associated with prolonged weightlessness must be mitigated well beyond our current capabilities (White and Averner 2001, Clement et al. 2007, Paloski et al. 2009). Indeed, in over 50 years of human spaceflight experience, including numerous long-duration missions (>3 months), not any single countermeasure or combination of countermeasures has been completely effective (Clement et al. 2007, Paloski et al. 2009). Current operational countermeasures have not been rigorously validated and have not fully protected long-duration (>3 months) crews in low-Earth orbit (Clement et al. 2007, Paloski et al. 2009). Thus, it seems unlikely that current countermeasures will adequately protect crews journeying to Mars and back over a three-year period particularly in the space environment where emergency medical treatments are still unknown and will be limited to crew capabilities. Therefore, a complete research and development program aimed at substituting for the missing gravitational cues and loading in space is warranted (Paloski et al. 2009). Virtually all identified risks associated with bone loss, cardiovascular deconditioning, muscle weakening, neurovestibular

disturbances, space anemia, and immune compromise might be alleviated by the appropriate application of artificial gravity (Clement et al. 2007, Paloski et al. 2009).

This document will focus on a basic study to aid in developing artificial gravity as a spaceflight countermeasure to physiological deconditioning, more particularly cardiovascular deconditioning. Cardiovascular deconditioning begins with the shifting of fluid from the legs and lower trunk to the head and chest immediately upon insertion into orbit. This produces the first symptoms of fullness of the head and associated discomfort on orbit and initiates an early loss of body fluid, including blood plasma (Buckey 2006). The relative excess of red blood cells is countered by arrested red cell production in the bone marrow and destruction of young red blood cells (Buckey 2006). The cardiovascular regulatory system that acts to maintain adequate blood pressure when we stand up on Earth is no longer needed in space and shows signs of deterioration (Fritsch-Yelle et al. 1994). Neither the fluid loss nor the loss of cardiovascular regulation and tone normally cause difficulties in orbit. During return to Earth, however, the renewed exposure to gravity can cause weakness and fainting. In addition, cardiovascular fitness is compromised post-flight, resulting in a diminished oxygen consumption capability during exercise (Levine et al. 1996). This is most likely because of reduced intravascular blood volume, stroke volume, and cardiac output resulting from space flight (Levine et al. 1996).

## Scientific Problem

During prolonged exposure to microgravity, gradual deconditioning occurs in the cardiovascular system, skeletal muscles, and bone, despite rigorous exercise during flight (Clement et al. 2007, Paloski et al. 2009). Cardiovascular deconditioning is a serious effect which includes decreased work capacity, reduced blood volume, impaired baroreceptor reflexes, and reduced orthostatic tolerance (Fritsch-Yelle et al. 1994, Buckey et al. 1996). These changes greatly limit an astronaut's ability to stand upright and/or perform normal daily activities after returning to the full gravity of Earth and may constitute a problem for Mars explorers who will have been without gravity for about a year in their journey from Earth. Astronauts commonly exhibit presyncopal and/or syncopal symptoms upon returning from spaceflight of various durations. Approximately 20-60% of astronauts (Buckey et al. 1996, Fritsch-Yelle et al. 1996) returning from short-duration (4-18 day) spaceflights and up to 83% of astronauts returning from long-duration (>1 month) spaceflights become presyncopal during postflight orthostatic challenges (Meck et al. 2001). As spaceflights become longer in preparation for possible human exploration of other planets, such as Mars, the deleterious effects of prolonged microgravity could pose a very serious threat to astronauts after they land, especially in the event of an emergency landing. Considerable research effort has been directed toward developing countermeasures, in addition to exercise, that can prevent or more effectively attenuate the deleterious changes. One countermeasure being tested is the application of intermittent artificial gravity provided by centripetal acceleration of a human via centrifuge. Intermittent artificial gravity via centrifugation has been shown to be beneficial in previous studies of ambulatory (Evans et al. 2004, Stenger et al. 2007) and bed-rested (Stenger et al. 2012) subjects. However, artificial gravity protocols have not been optimized for the cardiovascular system, or any other physiological system for that matter. Before artificial gravity protocols can be optimized for the cardiovascular system, cardiovascular

responses to the variables of artificial gravity need to be quantified. Variables of artificial gravity via centrifuge include radius of rotation ( $G_z$  gradient), rate of rotation (G-level), exercise state, and leg position.

### **Original Scientific Contribution**

This document will evaluate the effect of centrifuge radius ( $G_z$  gradient), with and without cycle ergometer exercise, on the cardiovascular systems of healthy male volunteers. Exercise was relatively constant in this study; however, exercise level can be a variable as well, by varying intensity and duration. Electrical impedance plethysmography was used to quantify segmental (thorax, abdomen, upper leg, lower leg) blood shifts and ECG was used to quantify heart rate. With knowledge gained from this basic study, artificial gravity variables can be constrained to optimize cardiovascular responses to centrifugation. By optimizing the cardiovascular responses, greater benefits should be possible from a countermeasure that has already shown benefits in terms of orthostatic tolerance.

## Chapter Two: Background

### Microgravity and Artificial Gravity

A person in an orbiting satellite or non-propelled spacecraft experiences a state of near-zero G-force commonly referred to as microgravity. Gravity from a nearby heavenly body acts on both the spacecraft and the person at the same time, thus both are pulled with exactly the same acceleratory forces and in the same direction. As result, the person is not attracted toward any specific wall of the spacecraft and simply floats “weightless” inside its chambers. Weight is decreased to nearly zero for much of a space mission; therefore the weight-bearing structures of the body are subject to a different set of stresses. Hydrostatic pressure gradients are changed along the body axes causing a fluid shift within the body (White and Averner 2001). The input to the body’s gravity receptors is also significantly altered (White and Averner 2001). Almost all of the body’s components and systems participate in the response to these events (White and Averner 2001).

Space biomedical researchers have been working for many years to develop countermeasures to reduce or eliminate the deconditioning associated with prolonged weightlessness. Despite these countermeasures, many astronauts experience problems with balance, orientation, and fainting during the first few days after landing (Paloski et al. 2009). They also risk muscle tears and bone fractures, thus must exercise an added degree of caution during their recovery period (White and Averner 2001). Given that the purpose of a human mission to Mars is not to go there and simply survive but rather to explore for scientific purposes, more effective countermeasures or combinations of countermeasures must be developed to address the effects of long-term exposure to microgravity (Clement et al. 2007). Astronauts arriving at Mars in a weakened physical condition with compromised immune systems who cannot

manage to ambulate would hardly be able to successfully execute an exploratory mission (Clement et al. 2007). They would be at risk in the event of bone fracture, alterations in the heart's rhythm, development of renal stones, or sensory-motor performance failure during piloting, extra-vehicular activity, or remote guidance tasks (Clement et al. 2007). Until the problems associated with microgravity exposure are overcome, such missions cannot be seriously considered (Clement et al. 2007).

Physical effects of spaceflight have been noted in astronauts and cosmonauts exposed to weightlessness for durations significantly less than those that will be experienced on exploratory class missions. These effects include loss of bone density, muscle mass, and red blood cells; cardiovascular, circulatory, and sensory-motor deconditioning; and changes in the immune system (Fritsch-Yelle et al. 1994, Buckey et al. 1996, White and Averner 2001, Buckey 2006, Clement et al. 2007, Paloski et al. 2009). Changes that occur after entering microgravity represent normal homeostatic responses to a new environment (Clement et al. 2007). The body's control systems recognize the lack of gravity and begin to adapt to this situation, not realizing that the ultimate plan is to return to normal gravity after a transient visit to microgravity. While such reactions may be appropriate in the microgravity environment, they are indeed quite inappropriate for return to Earth or arrival on the surface of another planet. These adaptive changes to weightlessness present a formidable obstacle to the human exploration of space, particularly for missions requiring travel times of several months or more. Such would be the case for a trip to Mars.

Countermeasures that address each of the physiological systems separately have shown only limited success. Over the 50 years of human space flight experience a variety of countermeasures have been developed, including saline loading, intermittent venous pooling (using lower body negative pressure, LBNP), pharmacological manipulations, and resistance training. All have had only limited success (Clement and Pavy-Le Traon 2004). The countermeasures

currently adopted to counteract the effect of microgravity conditions on board the International Space Station aim at stimulating particular physiological systems: the exercising treadmill and cycle ergometer for muscles (secondary for bone), and LBNP and fluid loading for cardiovascular responses (Clement and Pavy-Le Traon 2004).

One possible remedy that addresses multiple organ deconditioning is the application of artificial gravity because it influences most, if not all, physiological systems across the board. Rather than addressing each individual system in a piecemeal fashion, which is only valid if the principle of superposition holds for the combined effect of these interacting subsystems, artificial gravity stimulates all physiological systems simultaneously by simulating the natural 1G Earth gravitational environment (Clement et al. 2007). Artificial gravity offers a countermeasure with the possibility to address the debilitating and potentially fatal problems of bone loss, cardiovascular deconditioning (including fluid shift regulation and orthostatic hypotension), muscle weakening, sensory-motor and neurovestibular disturbances, and regulatory disorders (Clement et al. 2007, Paloski et al. 2009). Artificial gravity addresses all such systems, thus it can be considered as a multi-system or integrated countermeasure (Clement and Pavy-Le Traon 2004). The surest countermeasure is clearly one that produces a gravito-inertial environment close to that experienced on Earth (Clement et al. 2007).

Artificial (Earth-like) gravity can be created by accelerating or decelerating a spacecraft with a constant 1G linear acceleration, or by a 1G centripetal acceleration generated at the end of an arm rotating at a constant velocity. Generating a constant linear acceleration cannot be achieved by today's state of spacecraft propulsion. Centrifugation, however, is realistic and promises to be physiologically significant.

## Artificial Gravity via Centrifugation

From a physiological countermeasure perspective, a good solution may be to provide artificial gravity continuously throughout the mission. However, there are a number of engineering challenges associated with generating artificial gravity through the use of very large rotating vehicles or the application of very high linear acceleration, given the engines required to accomplish this. Such designs are not likely to be realized in the near future. In the case of a crewed Mars spacecraft, the structure required would be prohibitively large and certainly not energy efficient (Clement et al. 2007). A large rotating spacecraft presents serious design, financial, and operational challenges for a maneuvering station. Also, head movements and resultant Coriolis forces on a rotating spacecraft may limit the usefulness of centrifugation by generating motion sickness (Bukley et al. 2007).

An alternative approach being explored is to provide astronauts with a small spinning bed (see Figure 2.1 below). They would lie on their back with their head near the center of rotation and their feet pointing radially outward. Thus, their lower body could be loaded for a specified period of time each day in approximately the same way as under normal Earth gravity. While not expected to be as efficient as continuous artificial gravity from a physiological standpoint, given the gravity gradient effects and intermittent exposure, this procedure may prove effective. The engineering costs and design risks would certainly be lower as compared to designing a rotating spacecraft. From a practical perspective, it is likely that humans do not need gravity 24 hours a day to remain healthy (Vernikos 1997), thus a permanently rotating spacecraft would not be needed to produce a constant gravitational force. If intermittent gravity is sufficient, an onboard human short-arm centrifuge presents a realistic near-term opportunity for providing artificial gravity.



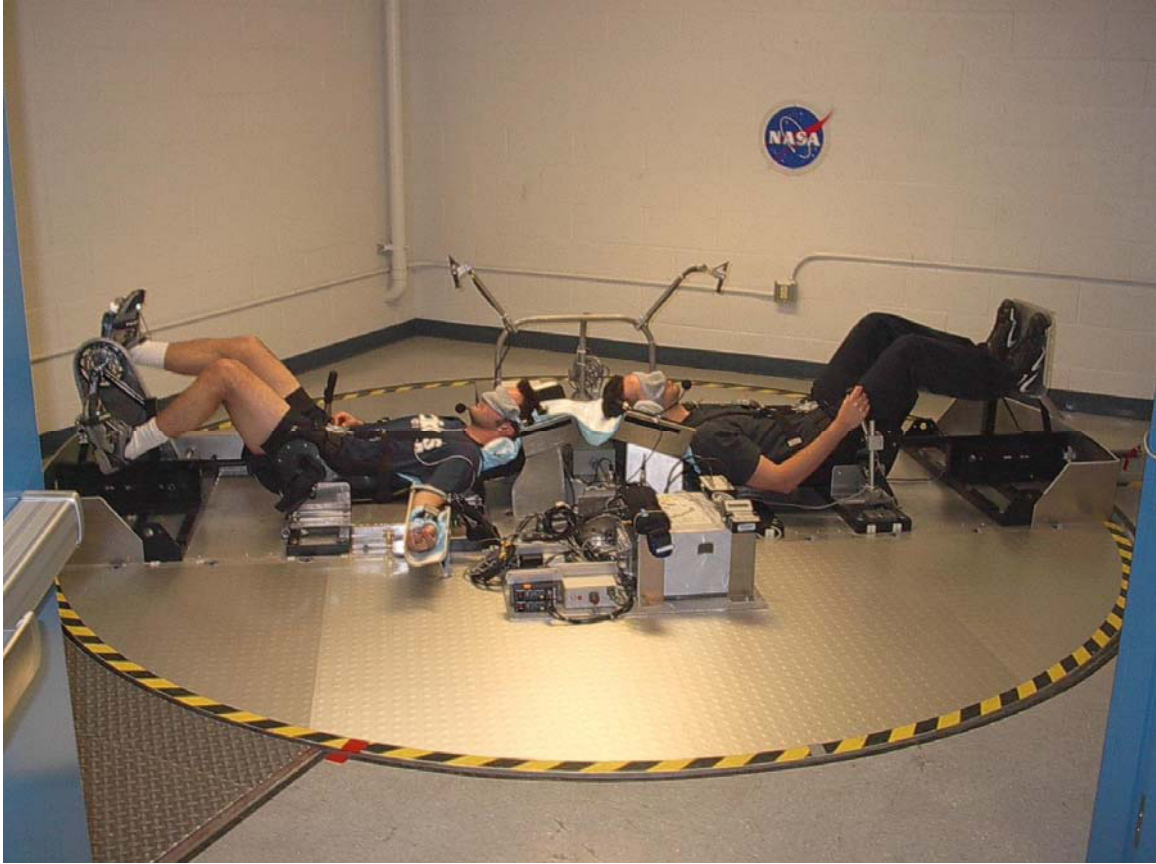


Figure 2.1: NASA Ames Human Powered Centrifuge (Stenger 2005).

The physiological responses associated with continuous exposure to an alternate gravity source such as Mars (0.38G) are unknown. In fact, human physiological responses to continuous exposure to anything other than 1G are unknown. If it turns out that substantial physiological deconditioning occurs in Mars gravity, then the application of artificial gravity may be required to protect crews during extended stays on the surface of Mars. The only feasible implementation on a planetary surface would be intermittent artificial gravity via a centrifuge (Clement et al. 2007).

On a centrifuge, artificial gravity is generated by centripetal acceleration. The amplitude of this acceleration varies directly with the radial distance from the center of rotation and with the square of rotational angular velocity. On a short-arm (~ 2 meters) centrifuge, the subject lies on his/her back on radius with the

head towards the center and the feet outwards, and the body perpendicular to the rotation axis. In this orientation, the centripetal acceleration is parallel to the body main axis and points toward the head (+G<sub>z</sub>, centrifugal force directed head-to-foot, see Figure 2.2 below). With a short-arm centrifuge there is a gravity gradient along the length of the body. Because the head is near the center, the G<sub>z</sub> level at the head is close to zero; but the G<sub>z</sub> can be upwards of two to four G's at the feet, depending on the rotational angular velocity.

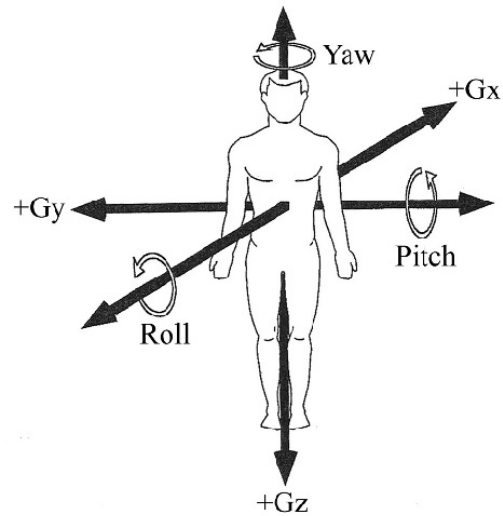


Figure 2.2: Cardinal axes of the human body (Clement and Bukley 2007).

## Physics of Artificial Gravity via Centrifugation

Artificial gravity is not gravity at all. Rather, it is an inertial force that is indistinguishable from the terrestrial gravitational field on Earth in terms of its action on any mass (Bukley et al. 2007, Paloski et al. 2009). In a rotating device, a centrifugal force proportional to the mass that is being accelerated centripetally is experienced rather than a gravitational attraction between bodies. Centrifugal force results from the centripetal acceleration generated by circular motion, or rotation. One can think of artificial gravity via centrifugation as the imposition of accelerations on a body to compensate for the forces that are absent in the microgravity of spaceflight (Bukley et al. 2007).

The forces ultimately exerted on the human body during centrifugation include the Coriolis force, gravity level, and gravity gradient. Reducing the centrifuge radius and increasing the rotation rate introduces potential problems associated with gravity gradient and Coriolis force. Although subjects at rest in a rotating system only feel the sensation of weight (gravity level generated by the centrifugal force), if they were to move, the Coriolis force would be felt. The Coriolis acceleration is dependent upon the angular velocity of the centrifuge and the linear velocity of the moving object, person, or body part. Coriolis force is independent of the radius of centrifugation and its magnitude is the same at all distances from the center of rotation. The Coriolis acceleration plays a significant role in causing the onset of motion sickness (Bukley et al. 2007). However, if the linear velocity is zero, then the Coriolis acceleration is zero.

For purposes in this document, the centripetal acceleration will be referred to as the gravity level. Circular motion is characterized by a radius and an angular velocity. The angular velocity is simply how fast the centrifuge is spinning. In a reference frame that is fixed to the rotating centrifuge, such that it is rotating along with the centrifuge, it appears as if an external force is pulling the subject toward the outer rim of the centrifuge. This centrifugal force is exerted on all objects in the rotating frame and is always directed away from the

axis of rotation towards the rim. Every stationary object within the centrifuge is forced away from the axis of rotation and the magnitude of this force is a function of the object mass, distance from the center of rotation, and the square of the angular velocity of the centrifuge. When a subject is lying on a short-arm centrifuge with his feet outward, the artificial gravity level at his feet is the product of radius at the feet and the square of the angular velocity.

The gravity level varies along the radius of the centrifuge, and a subject lying in a centrifuge along a radius with his feet positioned outboard will have his head closer to the axis of rotation than his feet. The head will have a smaller radius of rotation. Consequently, the gravity level at his head will be of lesser magnitude than the gravity level at his feet. The variation in artificial gravity level as a function of distance from the center of rotation is referred to as the gravity gradient. If the head is very close to the center of rotation a significant gravity gradient in the head-to-foot direction results.

## Ground-Based Artificial Gravity via Centrifugation

With the exception of the Neurolab (STS-90) mission (Clement and Pavy-Le Traon 2004), no actual data on the effects of artificial gravity induced by short-arm centrifugation during spaceflight exists. With Neurolab the hip was at the center of rotation, thus it provided effects different than centrifugation described in this document. The Visual and Vestibular Investigation System on Neurolab was utilized for ocular and vestibular research.

Notable differences exist between a centrifuge on Earth and in space. Both conditions generate a centripetal acceleration in the plane of rotation, but gravity is always present and perpendicular to the plane of rotation with the centrifuge on Earth. On Earth, gravity adds to the centrifugal force vectorially and produces a net gravito-inertial force that is tilted relative to the plane of rotation (see Figure 2.3 below). In space, the artificial gravity level is equivalent to the centripetal acceleration with direction aligned with the plane of rotation. The final assessment of an artificial gravity prescription via centrifugation can only be carried out in space.

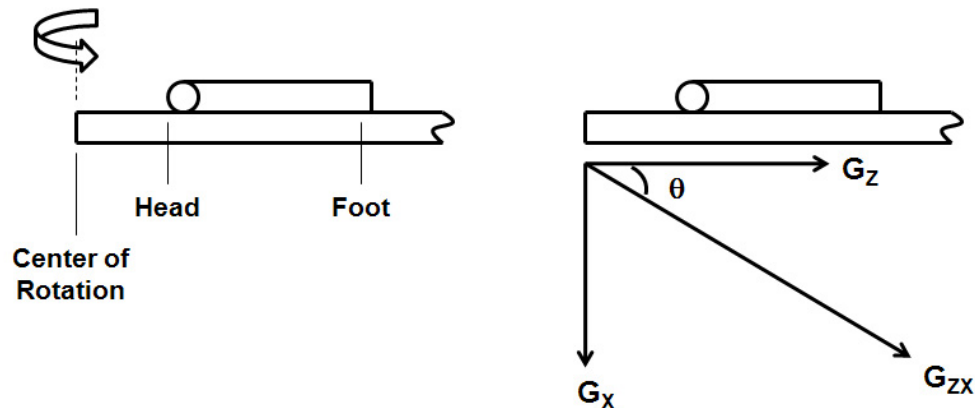


Figure 2.3: Centrifuge force vector diagram. Earth gravitational force ( $G_x$ ), centrifugal force ( $G_z$ ), net gravito-inertial force ( $G_{zx}$ ).

## Chapter Three: Specific Aims

### Rationale

Cardiovascular deconditioning is one deleterious effect from human spaceflight (exposure to microgravity) and includes decreased work capacity, reduced blood volume, attenuated baroreceptor reflexes, and reduced orthostatic tolerance (Buckey et al. 1996, Fritsch-Yelle et al. 1994, Fritsch-Yelle et al. 1996, Buckey 2006). These alterations can greatly limit an astronaut's ability to stand upright and/or perform normal daily activities after returning to the full gravity of Earth. In fact, astronauts commonly exhibit presyncopal and/or syncopal symptoms upon returning from spaceflight of various durations, including previously completed short duration (~10 days) Space Shuttle missions (Buckey et al. 1996). One countermeasure being tested is the application of intermittent artificial gravity provided by centripetal acceleration via centrifuge. Intermittent artificial gravity via centrifugation has shown to be beneficial in previous studies of ambulatory (Evans et al. 2004, Stenger et al. 2007) and bed-rested (Stenger et al. 2012) subjects. Physiological responses and/or changes have been cited as to why there is a potential benefit; however, mechanisms underlying the "why" are not understood (Evans et al. 2004, Stenger et al. 2007, Stenger et al. 2012). In addition, artificial gravity protocols have not been optimized for the cardiovascular system, or any physiological system for that matter. Before artificial gravity protocols can be optimized for the cardiovascular system, cardiovascular responses to the variables of artificial gravity need to be quantified, and mechanisms underlying the increased orthostatic tolerance from artificial gravity training need to be understood. This document proposes that a properly designed cardiovascular artificial gravity protocol for use during spaceflight will imitate the effects of the gravitational environment of Earth and will yield a net shift of blood from the thorax to the upper leg and lower leg

without detrimental accumulation of blood in the abdomen. This document operates under the premise that “pooling” of blood in the abdomen is undesirable for optimal maintenance of blood pressure homeostasis during gravitational challenges (Montgomery et al. 1977, Buckey et al. 1996, White et al. 1996, Arbeille P et al. 2008). It is anticipated that a properly designed protocol performed in microgravity will maintain the peripheral vasculature’s abilities at a level sufficient to facilitate venous return to the heart during orthostatic challenges upon return to a gravitational environment such as Earth.

The research presented in this document is intended to determine how the artificial gravity variables, radius (gravity gradient) and lower limb exercise, affect cardiovascular responses during centrifugation. Net fluid (blood) shifts between body segments (thorax, abdomen, upper leg, lower leg) will be analyzed to assess the cardiovascular responses to these variables of artificial gravity, as well as to begin to understand potential mechanism(s) underlying the beneficial orthostatic tolerance response resulting from artificial gravity training.

#### Specific Aim 1:

To determine how radial position along a centrifuge arm affects blood redistribution during centrifugation. The following hypothesis will be tested:

Hypothesis 1: Net fluid shift from the thorax will be greater for long radius without exercise (Protocol C, Figure 4.2) than for short radius without exercise (Protocol A, Figure 4.2).

### Specific Aim 2:

To determine how lower limb exercise affects blood redistribution during centrifugation. The following hypothesis will be tested:

Hypothesis 2: Net fluid shift from the thorax will be greater for short radius with exercise (Protocol B, Figure 4.2) than for short radius without exercise (Protocol A, Figure 4.2).

### Specific Aim 3:

To determine how radial position along a centrifuge arm and the resultant blood redistribution affect heart rate during centrifugation. The following hypothesis will be tested:

Hypothesis 3: Heart rates will be greater for long radius without exercise (Protocol C, Figure 4.2) than for short radius without exercise (Protocol A, Figure 4.2).

### Specific Aim 4:

To determine how lower limb exercise and the resultant blood redistribution affect heart rate during centrifugation. The following hypothesis will be tested:

Hypothesis 4: Heart rates will be greater for short radius with exercise (Protocol B, Figure 4.2) than for short radius without exercise (Protocol A, Figure 4.2).



## Chapter Four: Experiment Methodology

### Experimental Protocol Design Background

Exposure to some minimum level of G-force stimulus is probably essential to 1) maintain the body's physiological memory of vascular hydrostatic pressures, 2) maintain the afferent input required to sustain the integrity of neural regulatory functions, and 3) enhance the effectiveness of activity (exercise) on muscular health, strength and endurance, on aerobic work capacity, and bone integrity and strength (Vernikos 1997). It is not known what the profile and minimum requirements of exposure to G-forces would be in order to prevent deconditioning effects of microgravity and maintain Earth-like physiology. In general, physiological systems respond to signal and intensity change rather than to the duration of a stimulus, and shorter +Gz exposures would certainly work best from logistics, psychological and compliance perspectives (Vernikos 1997). In a study comparing effects of active versus passive standing, coupled with two versus four hours duration, as a countermeasure to simulated microgravity (head down bed rest), it was clear that the preventive value of active or passive +1Gz to head down bed rest-induced deconditioning is system specific since no one treatment was most effective across the responses tested (Vernikos 1997). The responses tested were orthostatic tolerance, peak VO<sub>2</sub>, plasma volume, and urinary Ca<sup>2+</sup> excretion. This suggests that both passive and active +Gz exposures should be built into any final gravitational countermeasure prescription (Vernikos 1997).

Many ground-based studies conducted with intermittent short-arm centrifugation have utilized centrifuges of ~6 ft radius (Greenleaf et al. 1996, Hastreiter and Young 1997, Evans et al. 2004, Stenger et al. 2007, Stenger et al. 2012). Cardiovascular implications of gravity gradient (provided by different radii of rotation) are lacking in these studies. A previous gravity gradient (provided by G-level) evaluation was performed at Massachusetts Institute of Technology

using a two meter centrifuge and three different G-levels (0.5, 1.0, and 1.5); heart rate, blood pressure, and calf volume were measured in this study (Hastreiter and Young 1997). They concluded that cardiovascular responses at 1.5G were statistically similar to standing during a timeframe of 30 minutes. Little is known concerning the effects of different gravity gradients (along the z axis) on the cardiovascular system of a human spinning on a centrifuge, at for example, two different radial positions. Basic data of this type is critical for the design of optimal artificial gravity countermeasures. To this end, the University of Kentucky's Center for Biomedical Engineering partnered with NASA Ames Research Center to conduct a pilot study utilizing the 29-foot radius NASA Ames 20G Centrifuge (Figure 4.1).

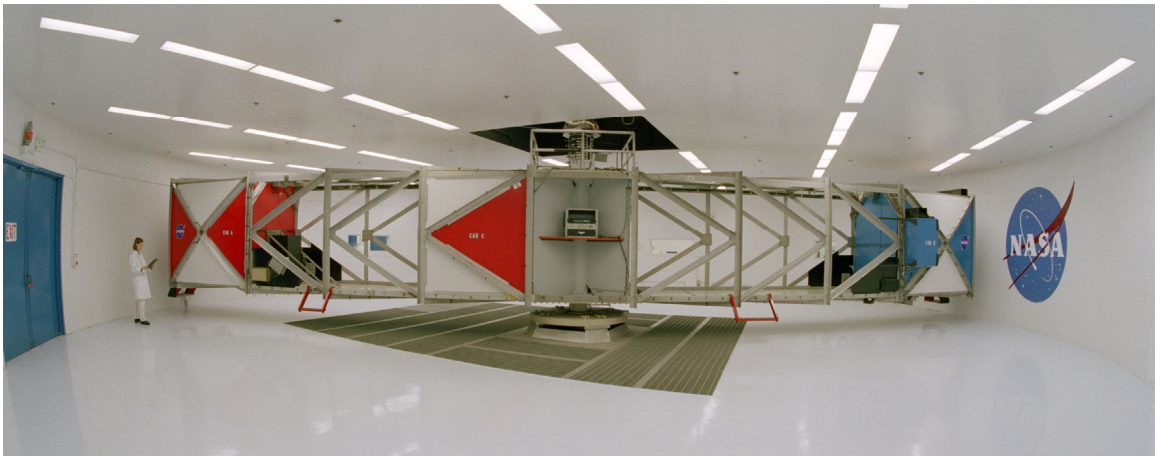


Figure 4.1: NASA Ames 20G Centrifuge.

## Experimental Protocols

The University of Kentucky / NASA Ames 20G study included six centrifuge protocols of which three (A, B, and C), were chosen for the current study (Figure 4.2 below). **Protocol A:** After 10 minutes of supine control, subjects were exposed to rotational 1  $G_z$  at a radius of rotation equal to 8.36 ft (2.54 m) for 2 minutes followed by 20 minutes alternating between 1 and 1.25  $G_z$ . After the 10 minute control and before the rest of the protocol, a familiarization spin to 1  $G_z$  was performed for all experiment runs for a few seconds. In some cases, subjects had not been on the centrifuge in weeks so the familiarization spin's purpose was to reorient them to the acceleration process. **Protocol B:** Same as **A**, but lower limb exercise (70%  $VO_2$  max) preceded ramps to 1.25  $G_z$ . **Protocol C:** Same as **A** but radius of rotation equaled 27.36 ft (8.33 m). Protocol A, short radius without exercise, will be referred in abbreviated form as SRC-. SRC is a common abbreviation for short radius centrifuge. Protocol B, short radius with exercise, will be referred to as SRC+. The "+" denotes with exercise whereas the "-" denotes without exercise. Protocol C, long radius without exercise, will be referred to as LRC-. LRC is a common abbreviation for long radius centrifuge.

To meet the specific aims of this document, emphasis was placed on the experimental protocol variables centrifuge radius (gravity gradient) and lower limb exercise provided during the solid line portions of Protocols A, B, and C (Figure 4.2). Near the end of the protocols, subjects changed leg position (dashed line portions in Figure 4.2). This document focuses on the legs extended posture (body weight supported by a bicycle seat) that occurred during the early duration of the protocols (solid line portions in Figure 4.2).

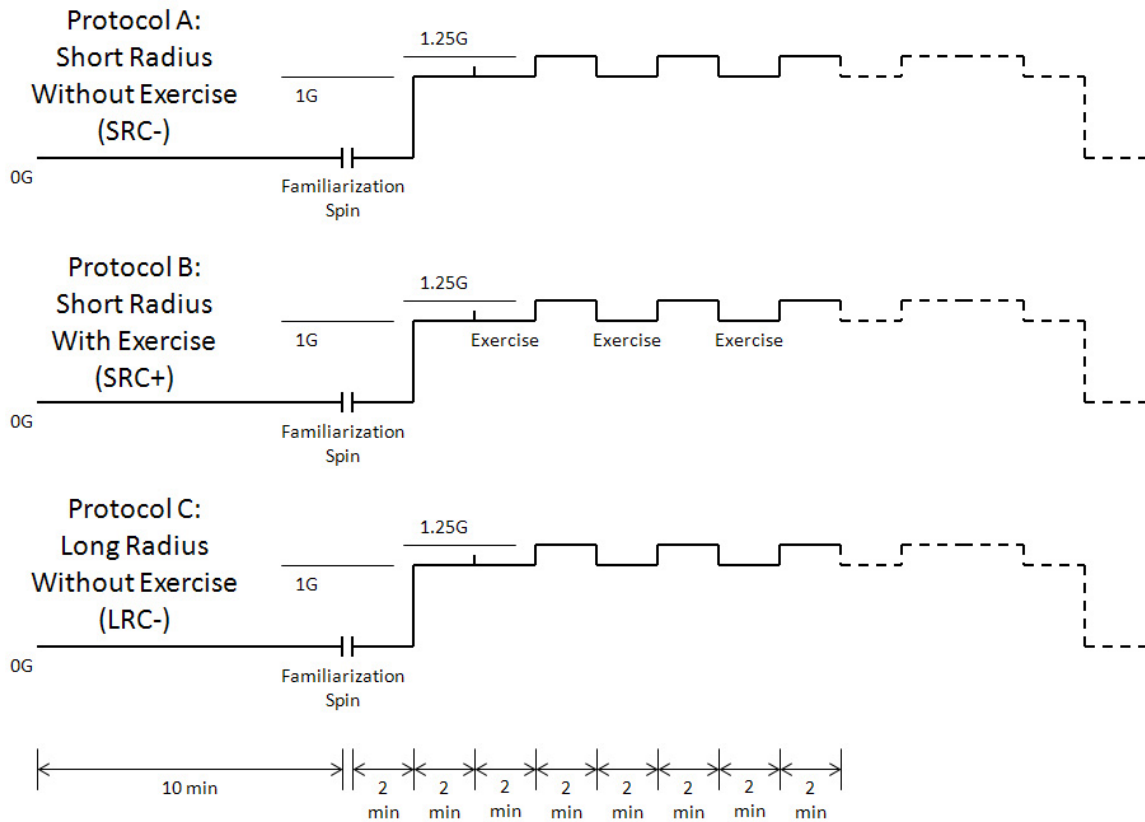


Figure 4.2: Centrifuge protocols A, B, and C.

The 1.25G upper limit was necessary due to the stress evoked by centripetal acceleration along the z axis at long radius. Two experienced centrifuge riders tested Protocol C at a level of 1.75G but this G-level was deemed intolerable and even caused petechiae at the ankles, caused by broken capillary blood vessels. The decision to lower the G-level to 1.25 was made for safety reasons and to ensure that all riders could complete Protocol C without suffering petechiae. One subject did not complete Protocol C due to presyncopal symptoms, but not petechiae. The G-level for Protocol A had to be adjusted accordingly so that Protocol A could be compared directly to Protocol C in order to learn about the radius effect.

In addition to Protocols A, B, and C, the subjects also experienced three other centrifuge protocols (D, G, and H) and one tilt test protocol over the

duration of the University of Kentucky / NASA Ames 20G Centrifuge study. Each protocol was performed on a different day for each subject. Data from these protocols are not presented here. Protocol D was the same as Protocol B but radius of rotation equal to 27.36 ft (8.33 m). Protocol G involved various G-levels (1G to 3G) and exercise at radius of rotation equal to 8.36 ft (2.54 m). Protocol H involved various G-levels (1G to 2.5G) and exercise at radius of rotation equal to 27.36 ft (8.33 m). Although the results are not presented here, blood was drawn from each subject before and after each centrifuge protocol.

## Evaluation of Experimental Protocols

A summary of radii, rotation rates,  $G_z$  levels, and  $G_z$  gradient slopes is given in Table 4.1 below, while the radii dimensions and  $G_z$  levels at the head and foot locations for short and long radius at 1G and 1.25G are shown below in Figure 4.3.

Table 4.1: Centrifuge radii, rotation rates,  $G_z$  levels, and slopes of  $G_z$  gradient.

	Radius at Head	Radius at Foot	Rate of Rotation	$G_z$ Level at Head	$G_z$ Level at Foot	Slope of $G_z$ Gradient
Short Radius	2.83 ft (0.86 m)	8.36 ft (2.54 m)	18.8 rpm	0.34G	1.00G	0.121 G/ft
			21.0 rpm	0.42G	1.25G	0.150 G/ft
Long Radius	21.83 ft (6.65 m)	27.36 ft (8.33 m)	10.4 rpm	0.80G	1.00G	0.037 G/ft
			11.6 rpm	1.00G	1.25G	0.046 G/ft

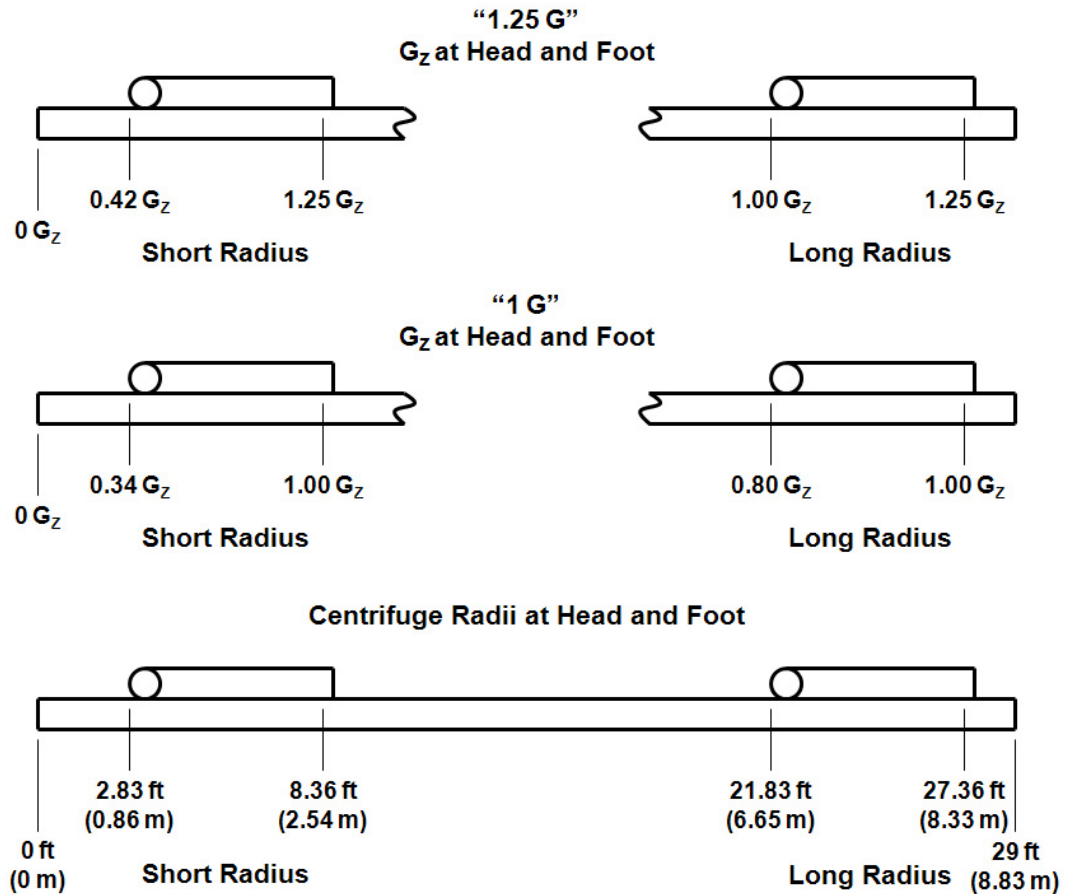


Figure 4.3: Centrifuge radii and G<sub>z</sub> levels at head and foot.

In Figure 4.4 below, gravity levels are plotted along the length of the body, allowing visualization of the G<sub>z</sub> gradients from head to foot for 1G and 1.25G, at short and long radius, experienced by subjects in protocols A, B, and C. It is important to note that although G<sub>z</sub> levels varied linearly from head to foot, the venous pressures within the body that dictated blood redistribution varied non-linearly from heart to foot. Increased gravitational force causes marked redistribution of blood volume in accordance with changes in transmural pressure (Rowell 1993). The venous transmural pressure is the sum of the dynamic pressure and the hydrostatic pressure (Rowell 1993). The hydrostatic pressure at any point in the circulation is determined by the height of the continuous

column of blood between that point and the heart (Rowell 1993). On Earth, the hydrostatic pressure varies linearly along the length of the body according to the formula  $\rho gh$ , where  $\rho$  is fluid density,  $g$  is acceleration due to gravity, and  $h$  is the height of the hydrostatic column. On a centrifuge, the hydrostatic pressure varies in a parabolic manner (in theory) due to the fact that acceleration ( $g$ ) varies according to radius which is the same as height of the column ( $h$ ).

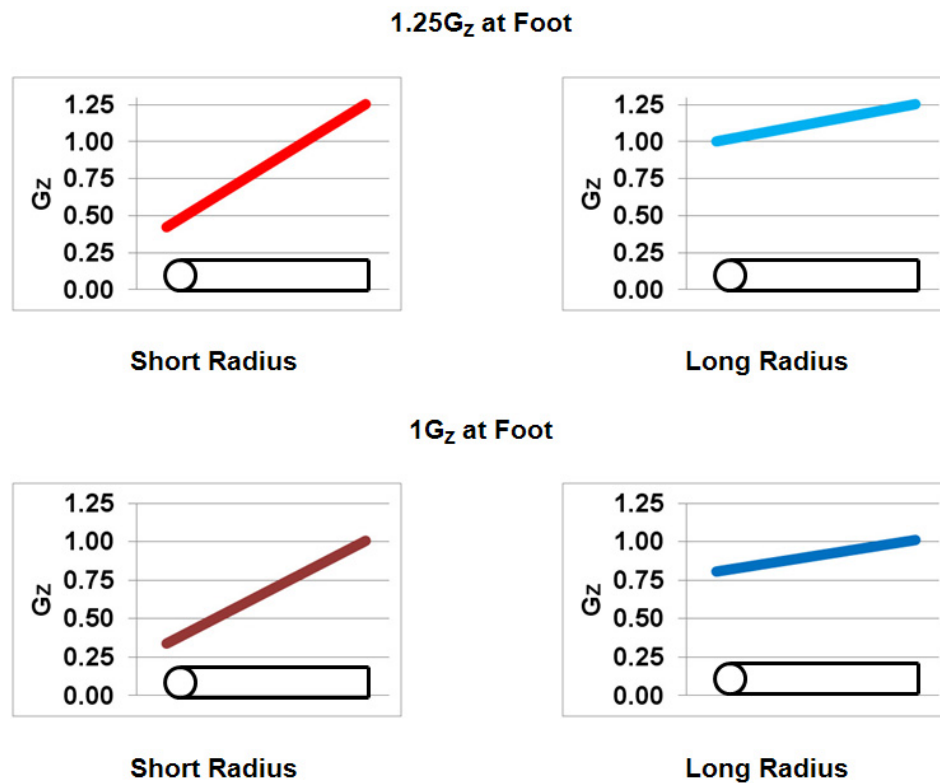


Figure 4.4: G<sub>z</sub> gradients from head to foot.



The physics of centrifugation on Earth must be kept in mind, thus Figure 4.5 below depicts the net gravito-inertial forces experienced by subjects in protocols A, B, and C.

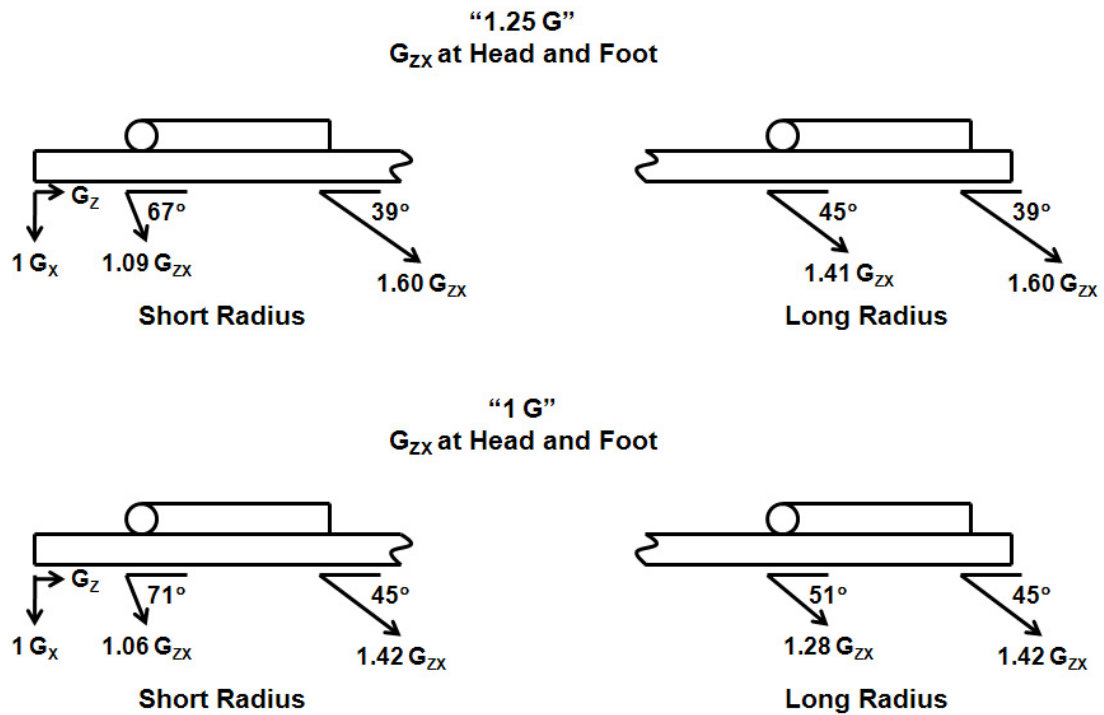


Figure 4.5: Net gravito-inertial forces ( $G_{ZX}$ ) at head and foot.

## Chapter Five: Data Analysis

### Subjects

Data were recorded from twelve healthy male volunteers who were screened for cardiovascular health as well as absence of tobacco, drug, and alcohol use. Female subjects were not selected for this pilot study because of the added difficulty of tracking menstrual cycles. The order in which subjects experienced the protocols was randomized; in addition, half of the subjects experienced short radius protocols first while the other half experienced long radius protocols first. The overall completion of the pilot study was under a time constraint imposed by the NASA Ames 20G facility and time would not have been available to ensure that females' menstrual cycles were synchronized as they experienced the protocols. The men were age 35 yr (SD 9) and weighed 82.8 kg (SD 7.9) or 182 lbs (SD 17). The studies were approved by the Institutional Review Boards of NASA Ames Research Center and the University of Kentucky. Data from eight subjects are presented in this document because four subjects did not complete all protocols (A, B, C, and D).

### Instrumentation

Subjects were instrumented with four body segment (thorax, abdomen, upper leg, lower leg) bio-electrical impedance (UFI THRIM 2994D) and a high-fidelity 12-lead ECG (CardioSoft). Current injecting electrodes for impedance were placed on the forehead and ankle. The current detecting electrodes were placed near anatomic landmarks for repeatability across subjects and test days. These were designated the thorax (supraclavicular area to immediately below the pectoral muscle and aligned with the nipple), the abdomen (immediately below

the pectoral muscle aligned with the nipple to the iliac crest along the inguinal crease), the upper leg (iliac crest along the inguinal crease to just above the knee), the lower leg (just below the knee to the ankle). High-quality Ambu® Blue Sensor Ag/AgCl electrodes were used for both impedance and the 12-lead ECG.

Figure 5.1 below shows the author monitoring initial measurements from an instrumented subject. Informed consent was given by the subject to take the photograph as an example of subject instrumentation. Data presented in this document include the legs extended position with the subject's body weight supported by a bicycle seat. Worth noting is the bundle of black shielded wires laying on the subject's lap. Included in this bundle are the 10 wires for the 12-lead ECG and the 10 wires for the bio-electrical impedance device. The wires were electrically shielded to prevent unwanted noise in the data signals. To the right of the subject's feet is the data acquisition system for transmitting the data signals from inside the centrifuge chamber to outside the centrifuge chamber. To the right of the subject's head is the 3-lead ECG device whose signal was used at the medical monitor's station. On the subject's forehead, one of the electrodes used for the bio-electrical impedance can be viewed. The blue straps over the subject's shoulder were part of the harness system for emergency evacuation purposes.



Figure 5.1: Subject instrumentation.

## Data Acquisition

An Ethernet bridge was used to remotely acquire the data output from each measurement device in a separate room from the centrifuge chamber. Each channel of data was acquired with a sampling frequency of 1000 Hz using DATAQ acquisition software. At the end of each session, data were then converted to MATLAB compatible files for analysis purposes.

## Mean Values

In some instances bio-electrical impedance is dissected into its resistive and reactive components; in others, the total impedance is measured (Geddes and Baker 1989). The segmental base resistance can be monitored to determine the relative degree of blood pooling taking place in a body segment (Montgomery et al. 1993). In order to track the relative changes in segmental blood volume, the resistance component from impedance was used. A background of electrical impedance plethysmography is provided in Appendix B along with related equations. To mitigate the impact of “noise” in the resistance data, a Butterworth low-pass filter was used (Appendix A). After filtering, data were down-sampled from 1000 Hz to 10 Hz. Mean values of resistance over steady-state segments of data were calculated using MATLAB and then input into Excel spreadsheets. These mean values of resistance were input into an expression to calculate percent change of volume (Equation B3, Appendix B). The percent change of body segment volumes were used as the inputs for the statistical software.

The 12-lead ECG package output mean heart rate as an optional variable through its own software (CardioSoft, Houston, Texas). A dedicated laptop was mounted on the centrifuge in order to collect and record 12-lead ECG signals.

## Statistics

Two-factor within-subjects repeated measures analysis of variance (ANOVA) was used to calculate significance using SAS software. The two factors were protocol and time and was a within-subjects design because each subject experienced all of the treatments.

In the SAS code, a mixed linear model approach was used, specifically using “PROC MIXED”. The PROC MIXED was specifically designed to fit mixed effects models and can model random and mixed effects data, repeated

measures, spatial data, data with heterogeneous variances, and autocorrelated observations. A mixed model is a statistical model containing both fixed effects and random effects and is predominantly used in research involving human and animal subjects. For method of estimation the default residual maximum likelihood was used and is based on a maximum likelihood estimation approach. This approach requires that the distribution of the dependent variable is normal (Gaussian). To ensure that the distribution of the dependent variable was indeed normal, stem leaf plots and normal probability plots were evaluated in SAS. Also, to ensure homogeneity of variance, scatter plots were evaluated for appearance of randomness. The stem leaf plots, normal probability plots, and scatter plots were all used as criteria for exclusion of individual data points. For computing the denominator degrees of freedom for the test of fixed effects, the Satterthwaite approximation was used. The table of the test of fixed effects included protocol, time, and the interaction of protocol and time.

Post-hoc analysis included Fisher's least significant difference method, where significance was accepted for  $p < 0.05$ . Fisher's least significant difference method is a two-step testing procedure for pairwise comparisons of several treatment groups. In the first step of the procedure, a global test is performed for the null hypothesis that the expected means of all treatment groups under study are equal. If this global null hypothesis can be rejected at the pre-specified level of significance, then in the second step of the procedure, one is permitted in principle to perform all pairwise comparisons at the same level of significance (although in practice, not all of them may be of primary interest). To counteract the potential problem inherent with multiple comparisons, the Bonferroni-Holm correction was utilized in this study as a semi-conservative approach. The Bonferroni correction controls the probability of false positives, ordinarily at the risk of increasing the probability of producing false negatives. This is also known as reducing the power. Thus, a uniformly more powerful test procedure is implementing the Bonferroni-Holm adjustment and is more suitable for a larger number of multiple comparisons.

## Data Selection

In analyzing data, focus was emphasized on specific portions of Protocols A, B, and C. These specific portions provided the segments of data that were used to calculate mean values. Figure 5.2 below depicts the data segments used for fluid shift calculations (depicted in red) while Figure 5.3 below depicts the data segments used for heart rate analysis (depicted in red). Data near G-level transitions were avoided in calculating these mean values. The strategic comparison of certain protocols allowed for comparison of the effects of centrifuge radius (gravity gradient) and of lower-limb exercise. In the SAS code described above, comparisons between protocols in which only one variable changed were made to give appropriate results. Protocol A (SRC-) was compared to Protocol C (LRC-) in order to determine the effect of radius length during passive (non-exercise) centrifugation. Protocol A (SRC-) was then compared to Protocol B (SRC+) in order to determine the effect of exercise at short radius.

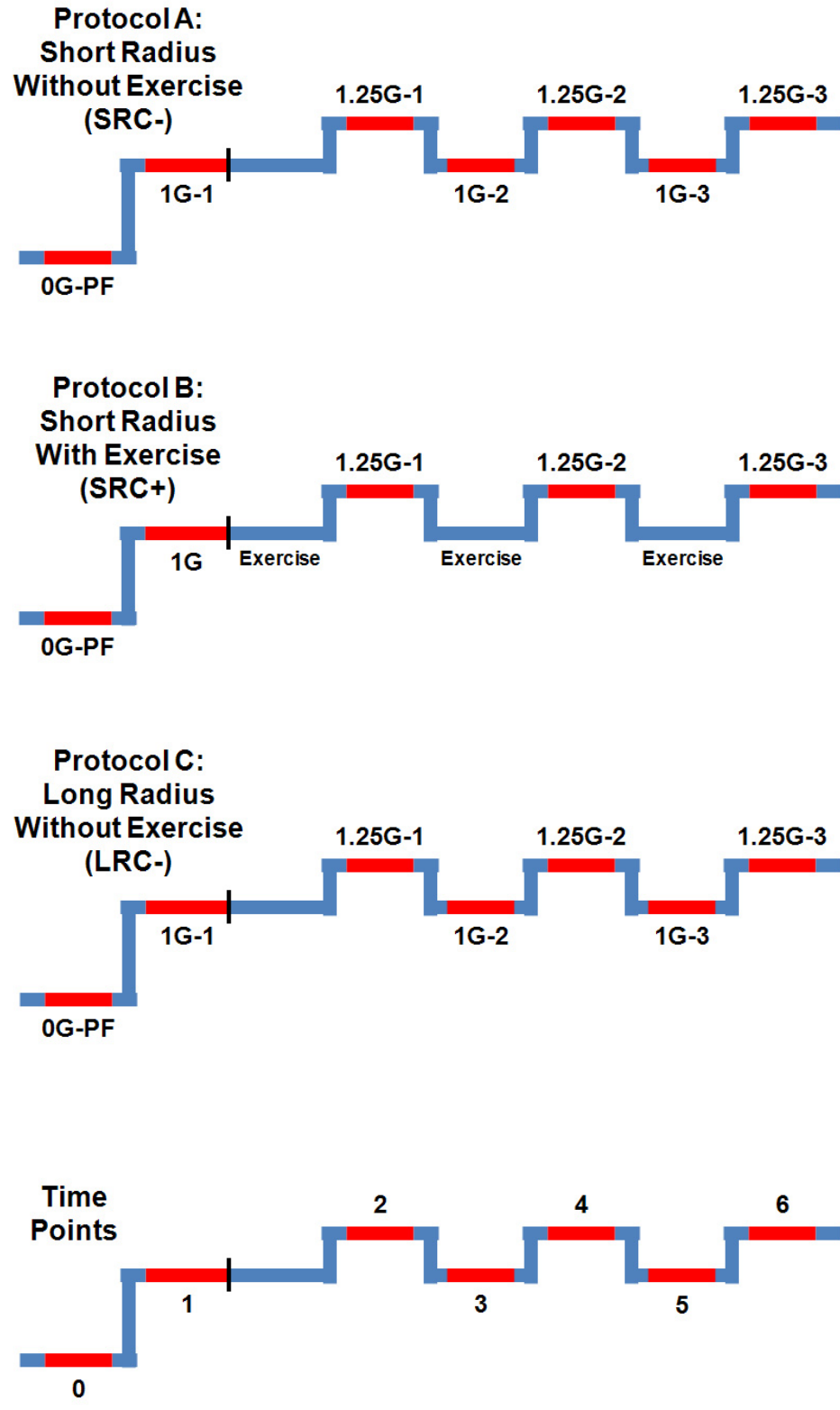


Figure 5.2: Fluid shift data segments (in red) and time point nomenclature for Protocols A, B, and C.



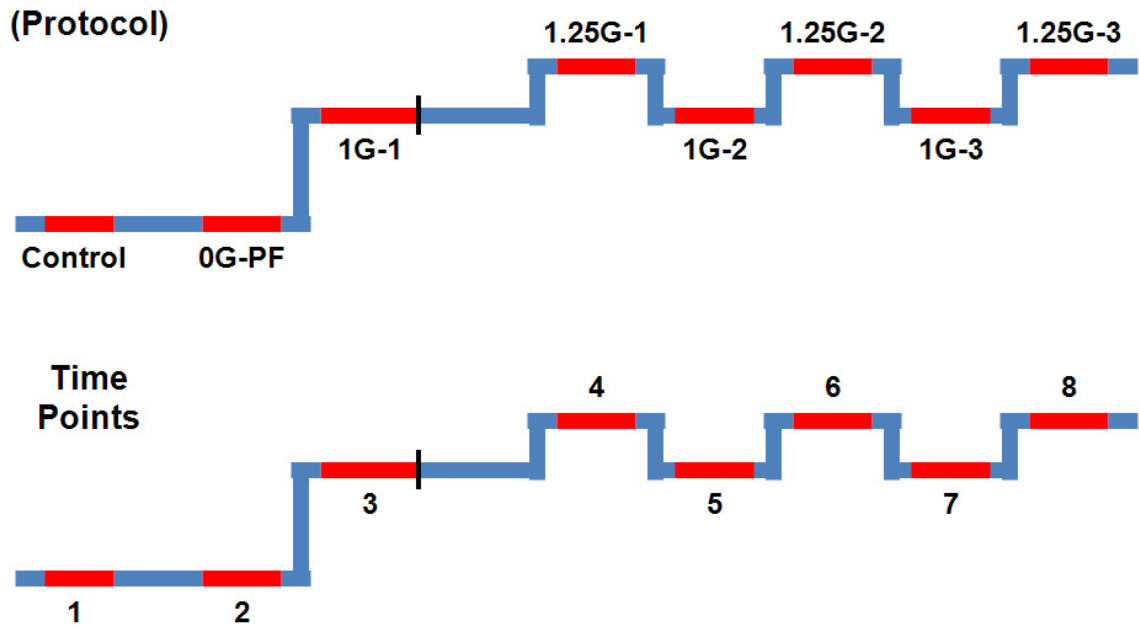


Figure 5.3: Heart rate data segments (in red) and time point nomenclature for Protocols A, B, and C.

## Chapter Six: Feasibility of Electrical Impedance Plethysmography Measurement

Protocol A (SRC-) was chosen for evaluation because it was the fundamental protocol upon which the other protocols were based. In the following figures a positive value represents a gain of fluid (blood) into a given region; whereas, a negative value represents a loss of fluid (blood) from a region of the body. Depicted below, Figure 6.1 shows group averaged  $\pm$  SE thoracic fluid shifts; whereas, Figure 6.2 shows individual subject responses that contributed to the average response. Figure 5.2 previously shown defines the time point nomenclature used in the fluid shift plots and tables.

As anticipated, a loss of fluid (-6 to -10%) occurred in the thoracic segment. Given the location of the thorax and the direction of the acceleration forces (Figure 4.5), it is intuitive that the thorax almost certainly had to lose fluid during +G<sub>z</sub> acceleration. The fluid loss most likely indicates a decreased thoracic venous blood volume, likely caused by a decrease in venous return. The fluid loss could also indicate a decrease of the reserve of blood that can be held in the respiratory system.

It is clear that a trend existed (not statistically tested) where thoracic fluid loss responded to G-level changes across the protocol (Figure 6.1). An initial loss of fluid (-6.7%) occurred during the first 1G segment (Time Point 1), followed by additional fluid loss (-8.5%) during the first 1.25G segment (Time Point 2). Throughout the protocol duration, fluid loss in the thorax oscillated in response to changing G-level. A positive relationship between greater fluid loss and higher G-level is intuitive and expected.

Another trend was also evident (not statistically tested) where thoracic fluid loss increased with time, both at the 1G and 1.25G segments. The stimulus was the same at each subsequent 1G and 1.25G segment. With the evaluation of the lower leg later, some of the additional fluid loss from the thorax was

accounted for by the additional fluid gain in the lower leg over time on the centrifuge. Also with time, the variability in the individual subject responses increased ( $\pm 0.4\%$  to  $\pm 1.1\%$ ).

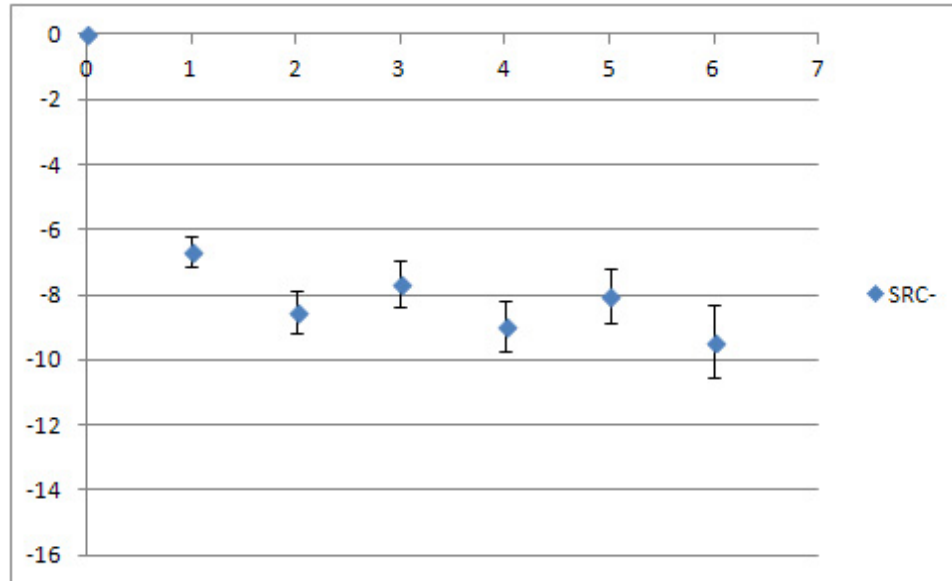


Figure 6.1: Average thoracic fluid shifts for SRC-. Values are means  $\pm$  SE.

Abscissa: Time Point (0 thru 6). Ordinate: Fluid Shift (%).

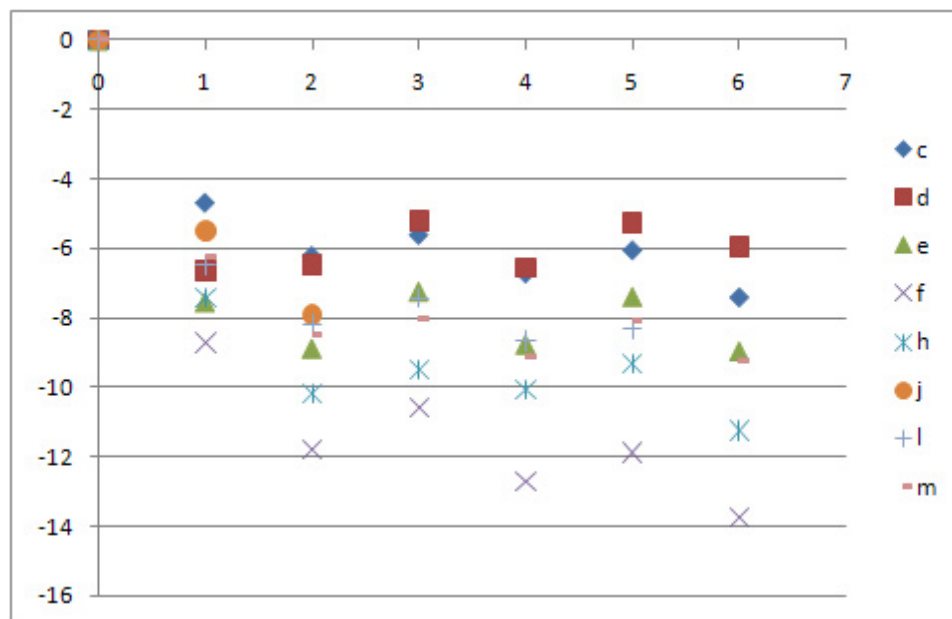


Figure 6.2: Individual subject thoracic fluid shifts for SRC-.

Abscissa: Time Point (0 thru 6). Ordinate: Fluid Shift (%).

The following figures depict fluid shifts into the abdomen. Figure 6.3 shows group averaged  $\pm$  SE abdominal fluid shifts; whereas, Figure 6.4 shows individual subject responses that contributed to the average response. The fluid gain most likely reflects increased venous blood volume. In the case of SRC-, the abdomen acted as a reservoir where blood pooled.

Unlike the thorax, the abdomen did not respond as clearly to changes in G-level between 1G and 1.25G. Also, unlike the thorax, the fluid change remained relatively constant (+5%) throughout the protocol. Similar to the thorax, the individual subject response variability increased over time ( $\pm 0.6\%$  to  $\pm 1.3\%$ ). Overall, the variability in the abdomen ( $\pm 1.0\%$ ) tended to be larger than in the thorax ( $\pm 0.7\%$ ).

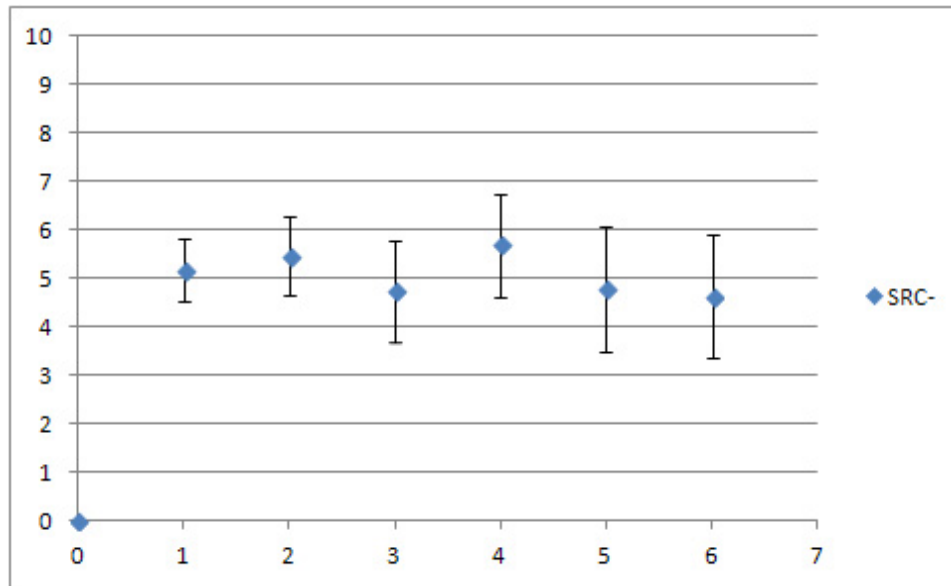


Figure 6.3: Average abdominal fluid shifts for SRC-. Values are means  $\pm$  SE.  
 Abscissa: Time Point (0 thru 6). Ordinate: Fluid Shift (%).

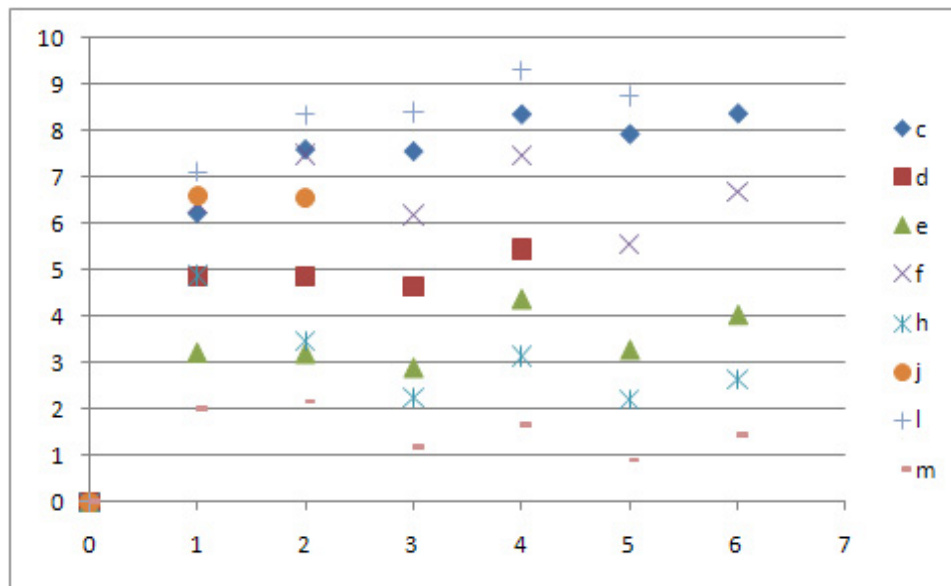


Figure 6.4: Individual subject abdominal fluid shifts for SRC-.  
 Abscissa: Time Point (0 thru 6). Ordinate: Fluid Shift (%).

The following figures depict changes in volume for the upper leg. Figure 6.5 shows group averaged  $\pm$  SE upper leg fluid shifts; whereas, Figure 6.6 shows individual subject responses that contributed to the average response. As depicted by the negative values, fluid loss occurred in the upper leg. The fluid loss most likely reflects decreased venous blood volume.

The fluid loss in the upper leg did not respond to changes in G-level and remained relatively constant (-2%) throughout the protocol. Compared to the variability shown previously in the thorax ( $\pm 0.7\%$ ), the variability of individual subject responses in the upper leg ( $\pm 1.0\%$ ) tended to be larger. Part of the increased variability is driven by the fact that one subject increased fluid volume whereas the other subjects lost fluid.

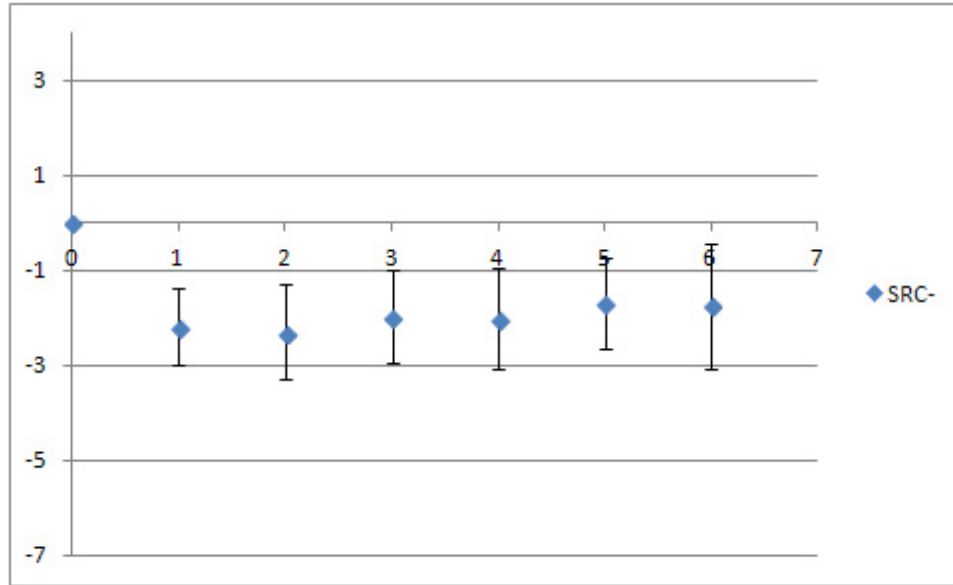


Figure 6.5: Average upper leg fluid shifts for SRC-. Values are means  $\pm$  SE.  
 Abscissa: Time Point (0 thru 6). Ordinate: Fluid Shift (%).

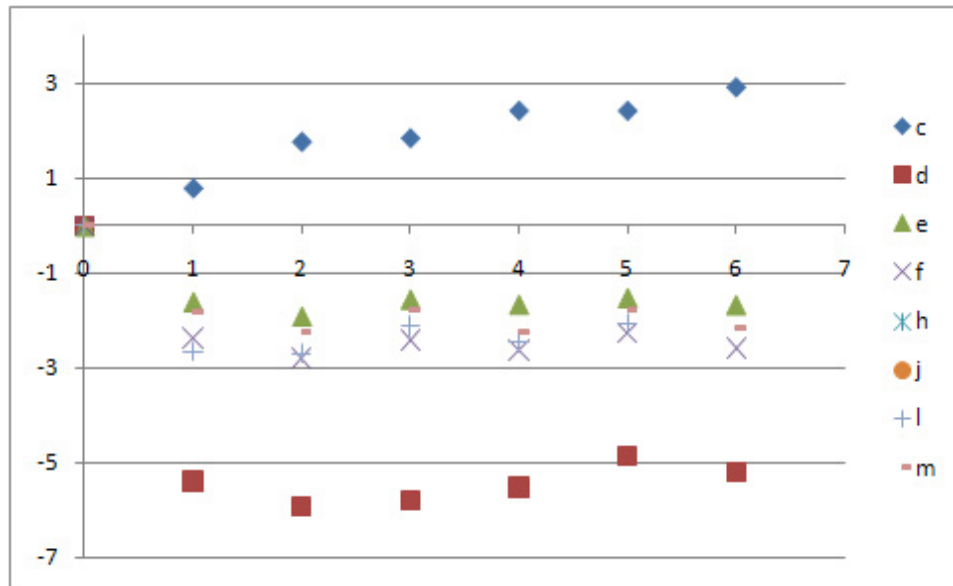


Figure 6.6: Individual subject upper leg fluid shifts for SRC-.  
 Abscissa: Time Point (0 thru 6). Ordinate: Fluid Shift (%).

The following figures depict volume changes for the lower leg. Figure 6.7 shows group averaged  $\pm$  SE lower leg fluid shifts; whereas, Figure 6.8 shows individual subject responses that contributed to the average response. As depicted by the positive values, fluid gain occurred in the lower leg. The fluid gain most likely reflects increased venous blood volume.

Unlike the thorax, the lower leg did not respond as clearly to changes in G-level except for the first 1G to 1.25G change. An initial gain of fluid (+1.8%) occurred during the first 1G segment (Time Point 1), followed by further (not statistically tested) fluid gain (+2.6%) that occurred during the first 1.25G segment (Time Point 2). More fluid gain at a higher G-level was expected. The variability of individual subject responses in the lower leg ( $\pm 0.6\%$ ) remained consistent over time and was comparable to the thorax ( $\pm 0.7\%$ ).



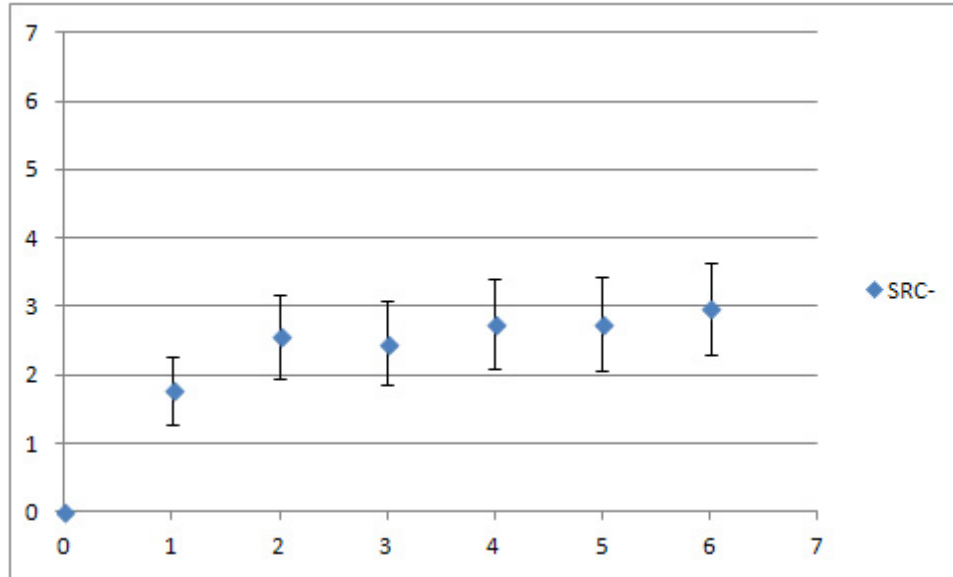


Figure 6.7: Average lower leg fluid shifts for SRC-. Values are means  $\pm$  SE.  
 Abscissa: Time Point (0 thru 6). Ordinate: Fluid Shift (%).

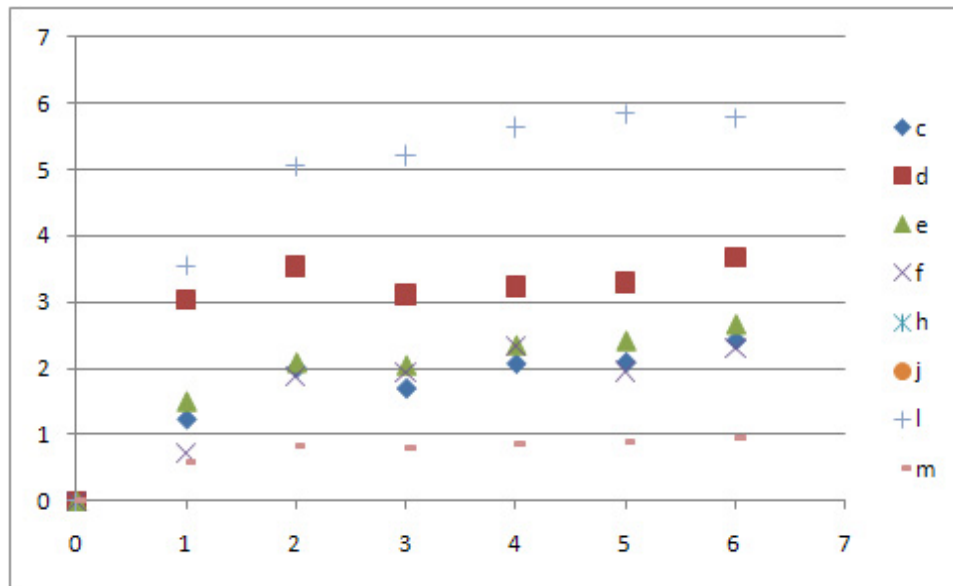


Figure 6.8: Individual subject lower leg fluid shifts for SRC-.  
 Abscissa: Time Point (0 thru 6). Ordinate: Fluid Shift (%).

The net resultant fluid redistribution (fluid loss vs. fluid gain) from SRC- is physiologically reasonable with average segmental fluid shifts of less than 10%. Thus it can be concluded that the electrical impedance plethysmography technique (described in theory and application in Appendix B) was successful at measuring fluid shifts during +G<sub>z</sub> acceleration. However, since no gold standard exists for quantifying fluid shifts between regions within the body, precise percent change in volume values have not been established. The impedance technique also has not been previously applied in a varying +G<sub>z</sub> centripetal acceleration environment. Fortunately, the impedance technique has been applied in a similar manner in studies using tilt tests as the method of +G<sub>z</sub> application.

A recent study published by Taneja and colleagues presented segmental (thoracic, splanchnic, pelvic, and leg) blood volume changes during 20°, 40°, and 70° upright tilt (Taneja et al. 2007). While the nomenclature for the segments is different from the present study, the anatomical placement of the detecting electrodes was nearly the same as the present study. The Taneja et al. study also used the same manufacturer of impedance monitor as in the present study. In the Taneja et al. study the subjects were tilted upright incrementally to 20°, 40°, and 70°, remaining at each angle for 10 minutes. In order to compare data from the present study to the Taneja study, tilt data from the present study were analyzed. The subjects that experienced SRC- also were briefly tilted upright at an angle of 70° on a different day. The first two minutes of data from the 70° tilt were analyzed in a similar fashion to that of SRC-. The fluid shifts from the present tilt study were: -11.2% for thorax, +6.5% for abdomen, +2.5% for upper leg, and +1.5% for lower leg (Figures 6.9 through 6.16 below). Interpretation from the plots provided by Taneja et al. yields: -7% to -12% for thoracic, +4% to +11% for splanchnic, +3% to +8% for pelvic, and +3% to +7% for leg volume changes. While not specified in the Taneja et al. publication, it is likely that the subjects stood on their feet during the upright tilt; whereas in the present study the subjects were supported by a bicycle seat to the extent that their feet did not support their bodyweight. It is also important to note that the tilt data from the

present study were two minutes in duration; whereas the Taneja et al. data were 10 to 30 minutes in duration. Despite these differences, the fluid shift results for the thorax and abdomen from the present study are in the range published by Taneja and colleagues. The upper leg and lower leg values from the present study are 0.5% and 1.5% respectively, below the range published by Taneja and colleagues. The upper and lower leg values could be low as result of less tilt time and/or by differing leg position during the tilt. A comparison of upright tilt data from the present study to that of published work by Taneja and colleagues provides credibility to the centrifuge percent change values obtained during 'SRC-'. The present study is the only of its kind to measure fluid shifts simultaneously in multiple body segments in subjects exposed to various acceleration stresses, thus no direct comparison exists in the published literature.

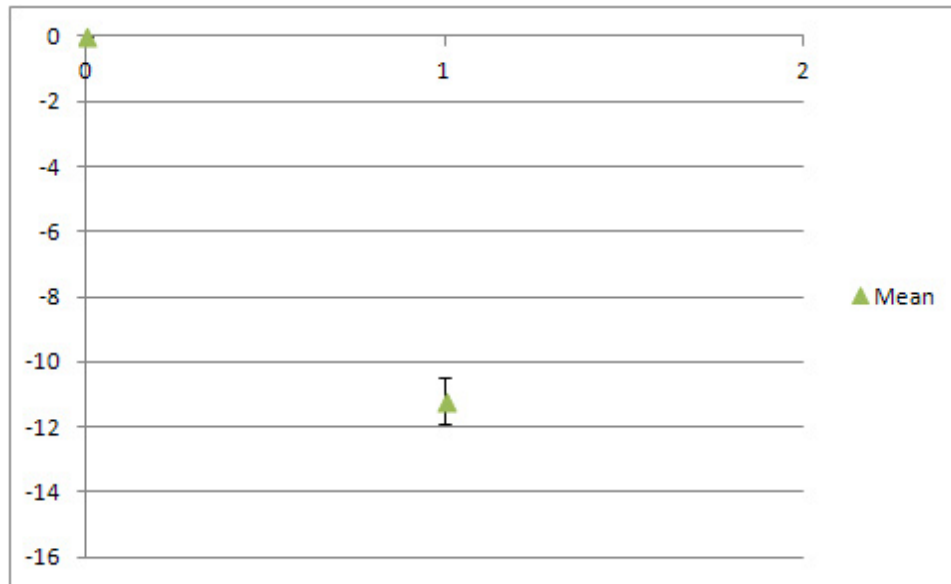


Figure 6.9: Average thoracic fluid shifts for 70° tilt. Values are means  $\pm$  SE.  
 Abscissa: Time Point (0 thru 1). Ordinate: Fluid Shift (%).

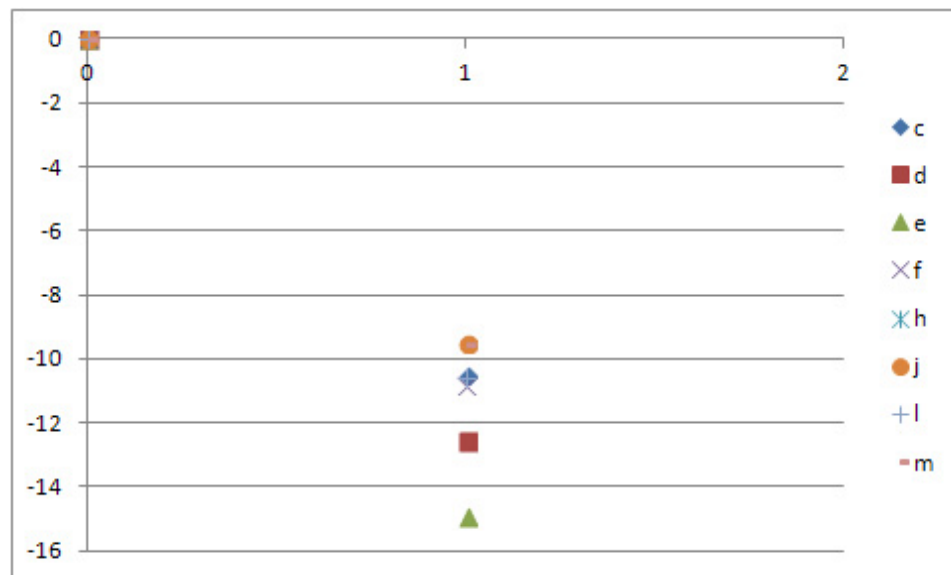


Figure 6.10: Individual subject thoracic fluid shifts for 70° tilt.  
 Abscissa: Time Point (0 thru 1). Ordinate: Fluid Shift (%).

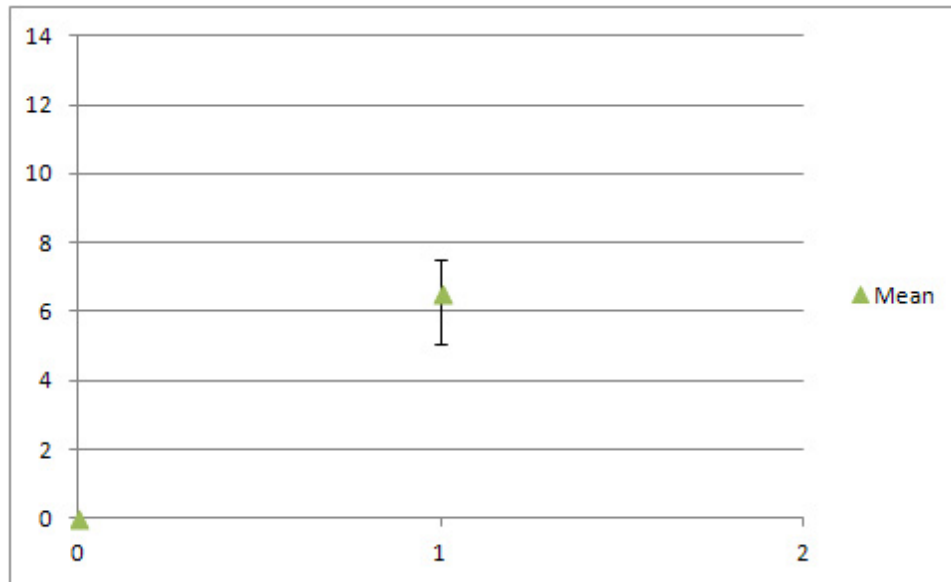


Figure 6.11: Average abdominal fluid shifts for 70° tilt. Values are means  $\pm$  SE.  
 Abscissa: Time Point (0 thru 1). Ordinate: Fluid Shift (%).

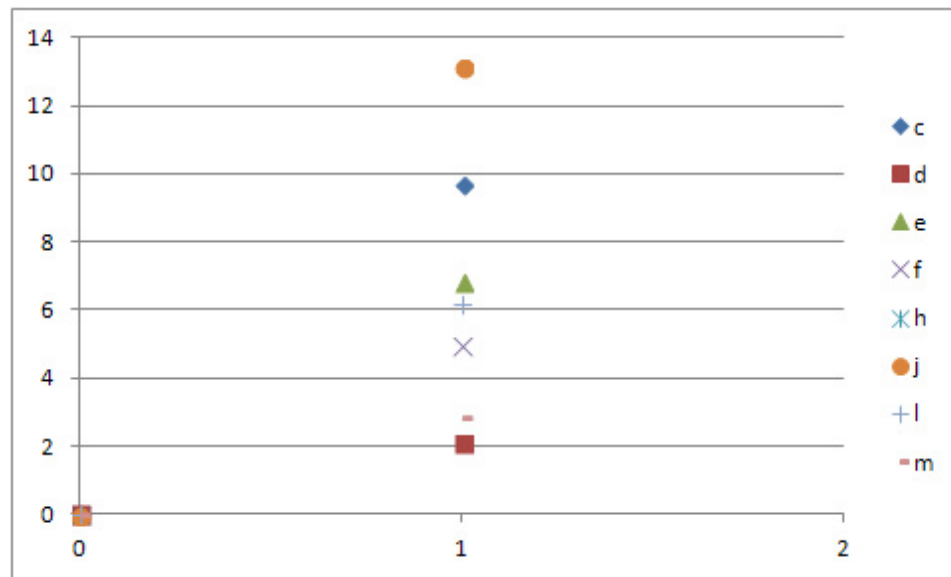


Figure 6.12: Individual subject abdominal fluid shifts for 70° tilt.  
 Abscissa: Time Point (0 thru 1). Ordinate: Fluid Shift (%).

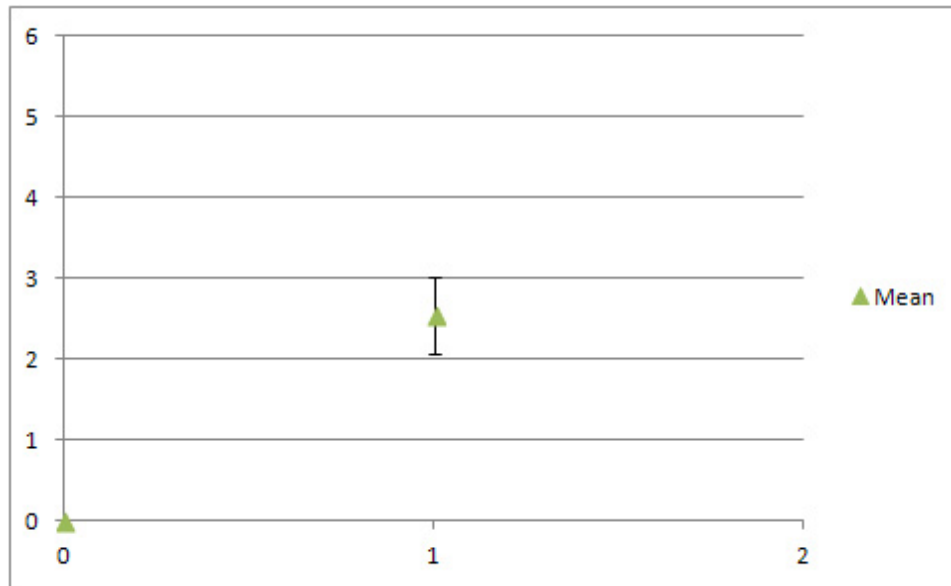


Figure 6.13: Average upper leg fluid shifts for 70° tilt. Values are means  $\pm$  SE.  
 Abscissa: Time Point (0 thru 1). Ordinate: Fluid Shift (%).

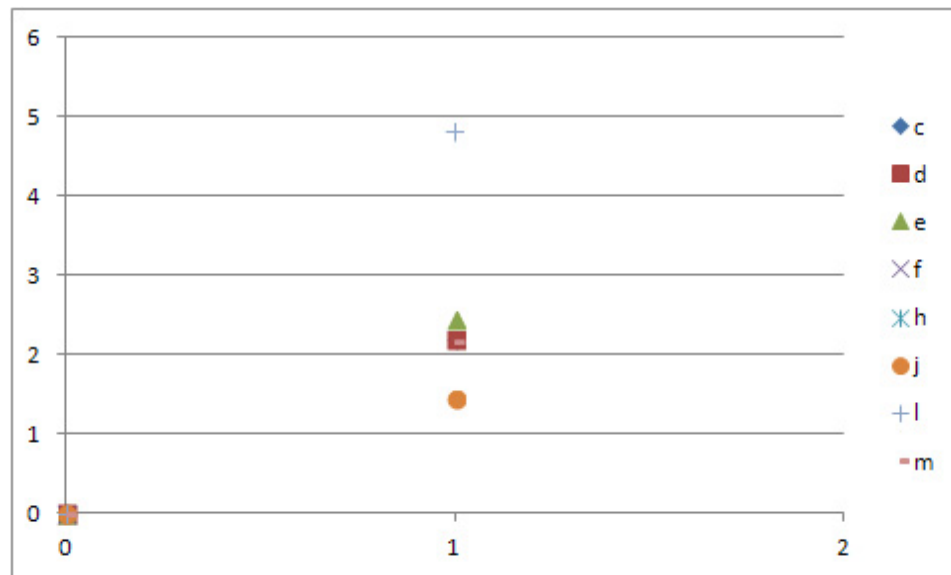


Figure 6.14: Individual subject upper leg fluid shifts for 70° tilt.  
 Abscissa: Time Point (0 thru 1). Ordinate: Fluid Shift (%).

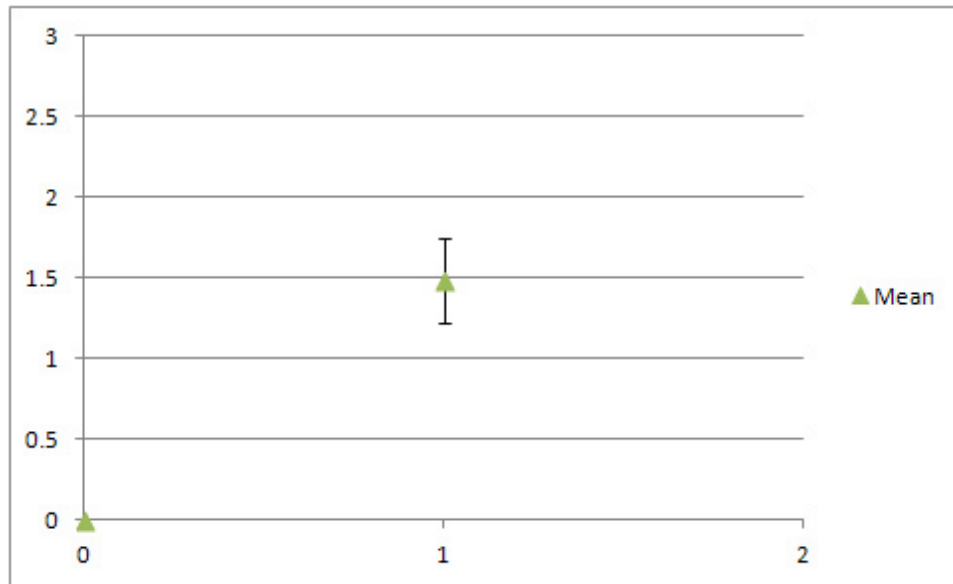


Figure 6.15: Average lower leg fluid shifts for 70° tilt. Values are means  $\pm$  SE.  
 Abscissa: Time Point (0 thru 1). Ordinate: Fluid Shift (%).

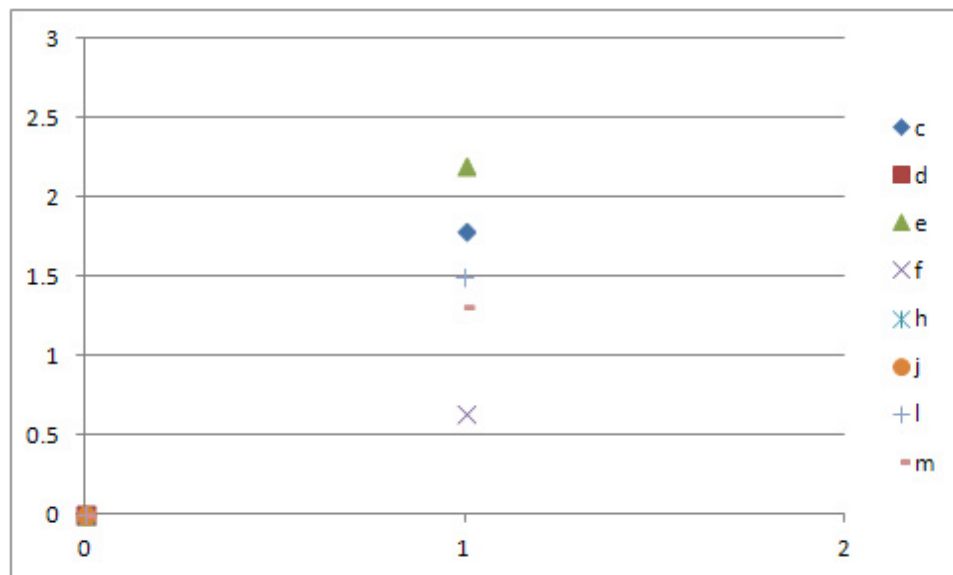


Figure 6.16: Individual subject lower leg fluid shifts for 70° tilt.  
 Abscissa: Time Point (0 thru 1). Ordinate: Fluid Shift (%).

## Chapter Seven: Results

### Specific Aim 1:

To determine how radial position along a centrifuge arm affects blood redistribution during centrifugation. The following hypothesis will be tested:

**Hypothesis 1: Net fluid shift from the thorax will be greater for long radius without exercise (LRC-) than for short radius without exercise (SRC-).**

The thoracic fluid shifts for LRC- were approximately 3% greater than for SRC-, but otherwise mirrored the SRC- response (Figure 7.1). The fluid shift trend oscillated in response to G-level with more fluid shift occurring at 1.25G than at 1G (not statistically tested).

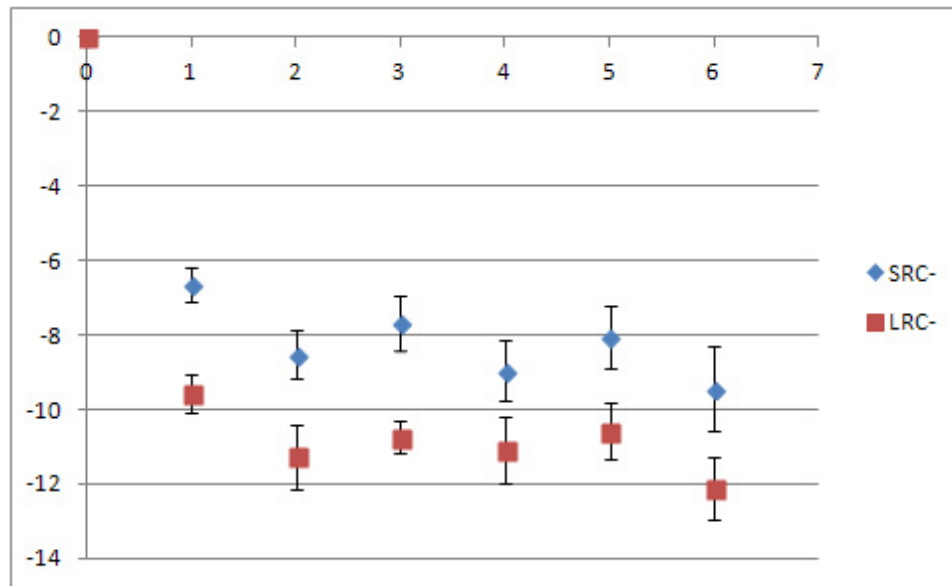


Figure 7.1: Thoracic fluid shifts SRC- versus LRC-. Values are means  $\pm$  SE.

Abscissa: Time Point (0 thru 6). Ordinate: Fluid Shift (%).



The main effect of protocol was significant at  $p = 0.0025$ . The fluid shifts away from the thorax for LRC- were significantly larger than for SRC- at all Time Points as shown in Table 7.1. The Fisher's procedure did not allow for pairwise comparisons to be valid due to the lack of a significant protocol by time interaction. However, after performing the Bonferroni-Holm procedure, the pairwise comparisons proved to be statistically significant.

Table 7.1: Thoracic fluid shifts SRC- (Protocol A) versus LRC- (Protocol C) statistical summary.

	SRC-	LRC-	p-value	BH p-value
A1	-6.7 ± 0.4	C1 -9.6 ± 0.5	0.002	0.007
A2	-8.5 ± 0.6	C2 -11.3 ± 0.9	0.002	0.004
A3	-7.7 ± 0.7	C3 -10.8 ± 0.4	0.001	0.007
A4	-8.9 ± 0.8	C4 -11.1 ± 0.9	0.003	0.003
A5	-8.0 ± 0.8	C5 -10.6 ± 0.8	0.002	0.005
A6	-9.4 ± 1.1	C6 -12.1 ± 0.8	0.001	0.007

A1 = Protocol A at Time Point 1. Values are means ± SE, units in %. BH = Bonferroni-Holm corrected p-value. Red indicates statistically significant p-values and/or BH p-values.

Similar in nature to the thoracic fluid shifts, the abdominal fluid shifts for LRC- mirrored the fluid shifts of SRC- with an approximate +2% baseline shift (Figure 7.2). Again, the fluid shift trend oscillated responding to the changing G-levels with more fluid shift occurring at 1.25G than at 1G (not statistically tested).

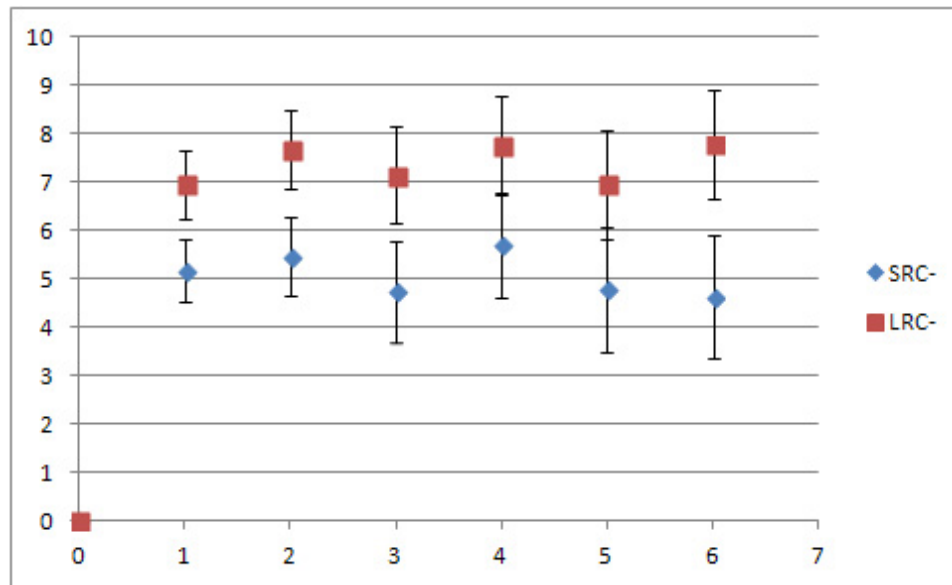


Figure 7.2: Abdominal fluid shifts SRC- versus LRC-. Values are means  $\pm$  SE.

Abscissa: Time Point (0 thru 6). Ordinate: Fluid Shift (%).

The main effect of protocol was nearly significant at  $p = 0.07$ . The fluid shifts into the abdomen for LRC- were not significantly larger than for SRC- at any of the Time Points as shown in Table 7.2. Compared to the thorax, the abdominal fluid shifts had greater variability, which is likely the major contributing factor for lack of statistical significance.

Table 7.2: Abdominal fluid shifts SRC- (Protocol A) versus LRC- (Protocol C) statistical summary.

	SRC-		LRC-	p-value	BH p-value
A1	5.2 ± 0.6	C1	7.0 ± 0.7	0.13	0.13
A2	5.5 ± 0.8	C2	7.7 ± 0.8	0.06	0.31
A3	4.7 ± 1.0	C3	7.1 ± 1.0	0.07	0.27
A4	5.7 ± 1.1	C4	7.8 ± 1.0	0.11	0.21
A5	4.8 ± 1.3	C5	7.0 ± 1.1	0.08	0.24
A6	4.6 ± 1.3	C6	7.8 ± 1.1	0.05	0.31

A1 = Protocol A at Time Point 1. Values are means ± SE, units in %. BH = Bonferroni-Holm corrected p-value. **Red** indicates statistically significant p-values and/or BH p-values.

Once again the fluid shifts for LRC- mirrored that of SRC- as shown for the upper leg (Figure 7.3) with an approximate +0.5% baseline shift. Again, the fluid shift trend oscillated (not statistically tested) responding to the changing G-levels; however, in the upper leg the overall trend moved gradually towards zero over time.

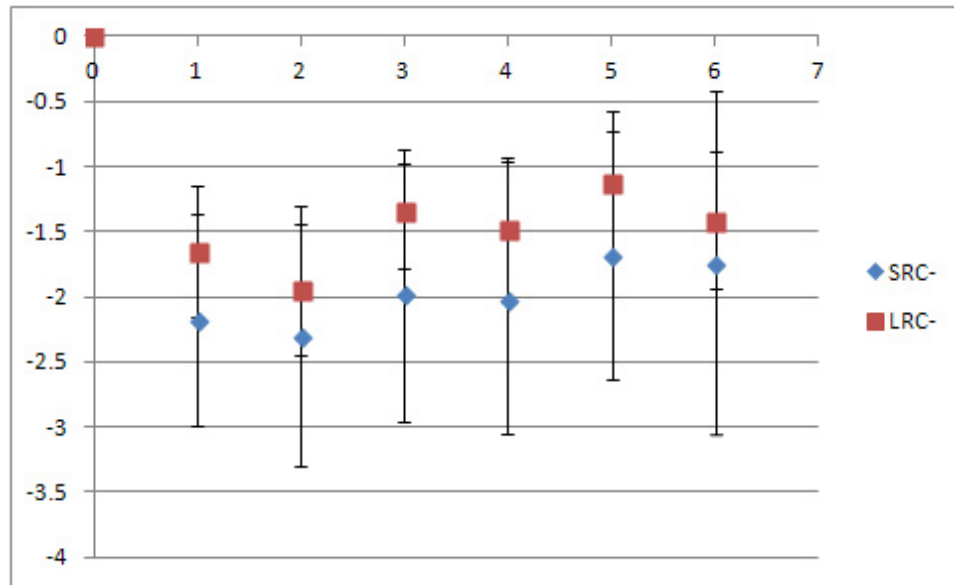


Figure 7.3: Upper leg fluid shifts SRC- versus LRC-. Values are means  $\pm$  SE.

Abscissa: Time Point (0 thru 6). Ordinate: Fluid Shift (%).

The main effect of protocol was not significant at  $p = 0.35$ . The fluid shifts from the upper leg for LRC- were not significantly different than for SRC- at any of the Time Points as shown in Table 7.3. The values for LRC- were not different from SRC- and there was also a large degree of variability in relation to the actual fluid shift values.

Table 7.3: Upper leg fluid shifts SRC- (Protocol A) versus LRC- (Protocol C) statistical summary.

	SRC-		LRC-	p-value	BH p-value
A1	-2.2 ± 0.8	C1	-1.7 ± 0.5	0.68	0.68
A2	-2.3 ± 1.0	C2	-1.9 ± 0.5	0.46	0.92
A3	-2.0 ± 1.0	C3	-1.3 ± 0.5	0.30	1.00
A4	-2.0 ± 1.0	C4	-1.5 ± 0.5	0.37	1.00
A5	-1.7 ± 1.0	C5	-1.1 ± 0.6	0.19	1.00
A6	-1.7 ± 1.3	C6	-1.4 ± 0.5	0.25	1.00

A1 = Protocol A at Time Point 1. Values are means ± SE, units in %. BH = Bonferroni-Holm corrected p-value. **Red** indicates statistically significant p-values and/or BH p-values.

For the lower leg, the fluid shifts for LRC- were essentially the same as for SRC- (Figure 7.4).

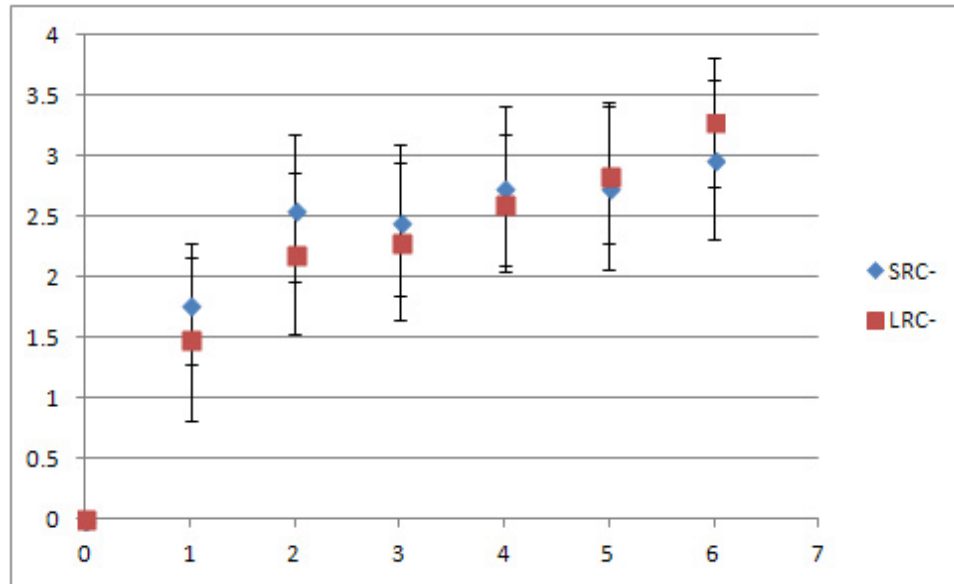


Figure 7.4: Lower leg fluid shifts SRC- versus LRC-. Values are means  $\pm$  SE.

Abscissa: Time Point (0 thru 6). Ordinate: Fluid Shift (%).

The main effect of protocol was not significant at  $p = 0.64$ . The percent change values were nearly identical at each Time Point with similar variability, thus no statistical differences (Table 7.4).

Table 7.4: Lower leg fluid shifts SRC- (Protocol A) versus LRC- (Protocol C) statistical summary.

	SRC-		LRC-	p-value	BH p-value
A1	1.8 ± 0.5	C1	1.5 ± 0.7	0.74	1.00
A2	2.6 ± 0.6	C2	2.2 ± 0.7	0.78	0.78
A3	2.5 ± 0.6	C3	2.3 ± 0.7	0.63	1.00
A4	2.7 ± 0.7	C4	2.6 ± 0.6	0.57	1.00
A5	2.7 ± 0.7	C5	2.8 ± 0.6	0.42	1.00
A6	3.0 ± 0.7	C6	3.3 ± 0.5	0.32	1.00

A1 = Protocol A at Time Point 1. Values are means ± SE, units in %. BH = Bonferroni-Holm corrected p-value. **Red** indicates statistically significant p-values and/or BH p-values.

## Specific Aim 2:

To determine how lower limb exercise affects blood redistribution during centrifugation. The following hypothesis will be tested:

**Hypothesis 2: Net fluid shift from the thorax will be greater for short radius with exercise (SRC+) than for short radius without exercise (SRC-).**

The nature of the fluid shifts from the thorax for SRC+ was completely different than for SRC- (Figure 7.5). The fluid shifts for SRC+ responded to the repetitive bouts of exercise.

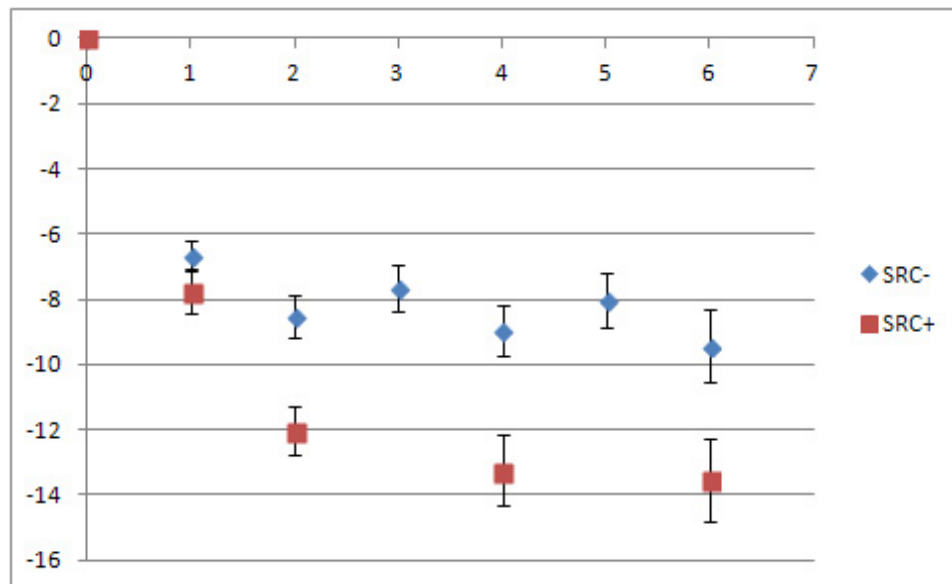


Figure 7.5: Thoracic fluid shifts SRC- versus SRC+. Values are means  $\pm$  SE.

Abscissa: Time Point (0 thru 6). Ordinate: Fluid Shift (%).



The main effect of protocol was significant at  $p = 0.0097$ . The thoracic percent change values were significantly different at each Time Point except for Time Point 1 (Table 7.5). SRC- and SRC+ both provided the same stimulus at Time Point 1, thus it was not expected to produce a different result.

Table 7.5: Thoracic fluid shifts SRC- (Protocol A) versus SRC+ (Protocol B) statistical summary.

	SRC-	SRC+	p-value	BH p-value
A1	-6.7 ± 0.4	B1 -7.8 ± 0.7	0.6942	0.6942
A2	-8.5 ± 0.6	B2 -12.0 ± 0.7	0.0071	0.0142
A3		B3		
A4	-8.9 ± 0.8	B4 -13.3 ± 1.1	0.0012	0.0036
A5		B5		
A6	-9.4 ± 1.1	B6 -13.5 ± 1.3	0.0009	0.0036

A1 = Protocol A at Time Point 1. Values are means ± SE, units in %. Data was not sampled at B3 and B5 due to the subjects exercising. BH = Bonferroni-Holm corrected p-value. Red indicates statistically significant p-values and/or BH p-values.

The nature of the fluid shifts into the abdomen for SRC+ was also completely different than for SRC- (Figure 7.6). SRC+ responded to the repetitive bouts of exercise with a decreased fluid shift amount (not statistically tested) from each subsequent bout of exercise.

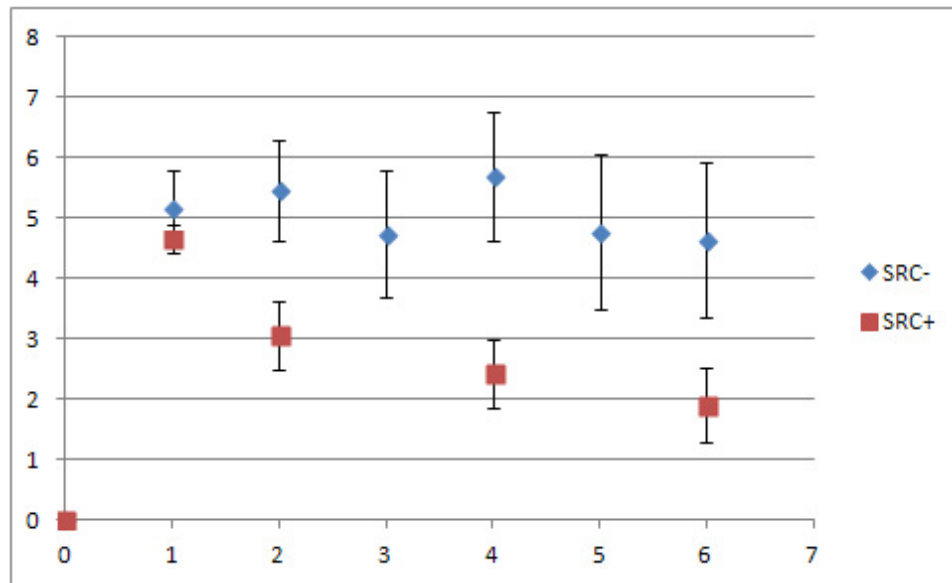


Figure 7.6: Abdominal fluid shifts SRC- versus SRC+. Values are means  $\pm$  SE.

Abscissa: Time Point (0 thru 6). Ordinate: Fluid Shift (%).

The main effect of protocol was significant at  $p = 0.0227$ . The percent change values were significantly lower for SRC+ at Time Points 4 and 6 (Table 7.6). The Bonferroni-Holm corrected p-value was not significant at Time Point 2 despite the uncorrected p-value being statistically significant.

Table 7.6: Abdominal fluid shifts SRC- (Protocol A) versus SRC+ (Protocol B) statistical summary.

	SRC-		SRC+	p-value	BH p-value
A1	5.2 ± 0.6	B1	4.6 ± 0.2	0.4372	0.4372
A2	5.5 ± 0.8	B2	3.1 ± 0.6	0.0314	0.0628
A3		B3			
A4	5.7 ± 1.1	B4	2.4 ± 0.6	0.0043	0.0172
A5		B5			
A6	4.6 ± 1.3	B6	1.9 ± 0.6	0.0048	0.0144

A1 = Protocol A at Time Point 1. Values are means ± SE, units in %. Data was not sampled at B3 and B5 due to the subjects exercising. BH = Bonferroni-Holm corrected p-value. Red indicates statistically significant p-values and/or BH p-values.

Again, the response for SRC+ was completely different than for SRC- as shown in the upper leg (Figure 7.7). The upper leg responded to the subsequent bouts of exercise with increasing amounts of fluid being shifted into the segment (not statistically tested), opposed to a loss of fluid as was the case with SRC-.

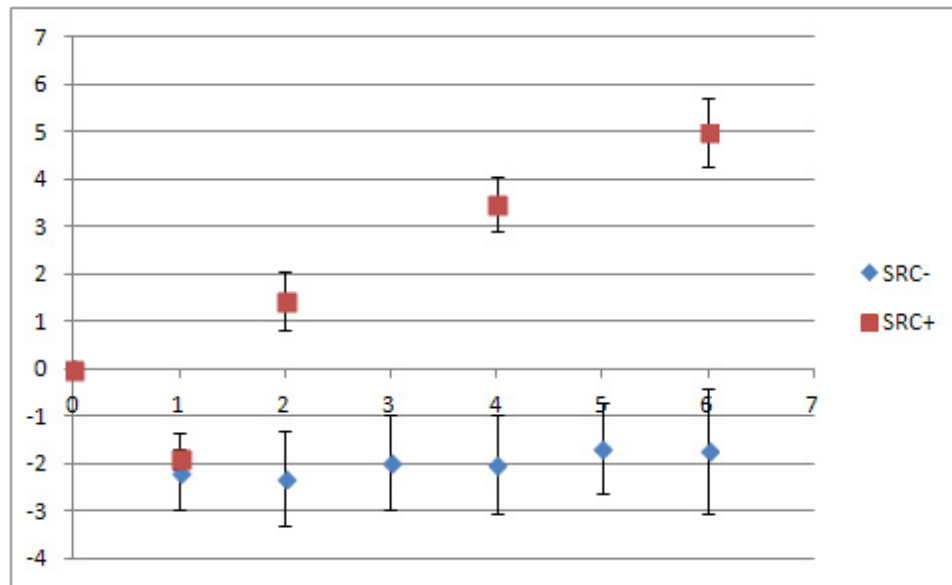


Figure 7.7: Upper leg fluid shifts SRC- versus SRC+. Values are means  $\pm$  SE.

Abscissa: Time Point (0 thru 6). Ordinate: Fluid Shift (%).

The main effect of protocol was significant at  $p = 0.0045$ . The percent change values were significantly different at all Time Points except for Time Point 1 (Table 7.7). The lack of difference for Time Point 1 was expected, as explained previously.

Table 7.7: Upper leg fluid shifts SRC- (Protocol A) versus SRC+ (Protocol B) statistical summary.

	SRC-		SRC+	p-value	BH p-value
A1	-2.2 ± 0.8	B1	-1.9 ± 0.2	0.7868	0.7868
A2	-2.3 ± 1.0	B2	1.4 ± 0.6	0.0063	0.0126
A3		B3			
A4	-2.0 ± 1.0	B4	3.5 ± 0.6	0.0006	0.0018
A5		B5			
A6	-1.7 ± 1.3	B6	5.0 ± 0.7	0.0001	0.0004

A1 = Protocol A at Time Point 1. Values are means ± SE, units in %. Data was not sampled at B3 and B5 due to the subjects exercising. BH = Bonferroni-Holm corrected p-value. Red indicates statistically significant p-values and/or BH p-values.

Similar to the upper leg, the fluid shift into the lower leg for SRC+ was different from SRC- (Figure 7.8) and responded to the subsequent bouts of exercise with increasing amounts (not statistically tested) of fluid being shifted into the segment.

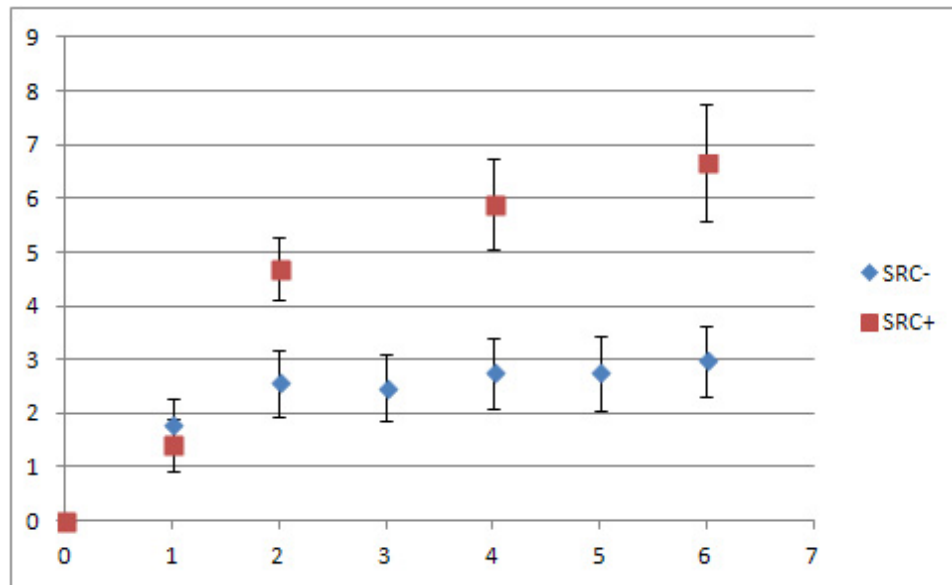


Figure 7.8: Lower leg fluid shifts SRC- versus SRC+. Values are means  $\pm$  SE.

Abscissa: Time Point (0 thru 6). Ordinate: Fluid Shift (%).

The main effect of protocol was significant at  $p = 0.0066$ . The percent change values were significantly different at all Time Points except for Time Point 1 (Table 7.8).

Table 7.8: Lower leg fluid shifts SRC- (Protocol A) versus SRC+ (Protocol B) statistical summary.

	SRC-		SRC+	p-value	BH p-value
A1	1.8 ± 0.5	B1	1.4 ± 0.5	0.8352	0.8352
A2	2.6 ± 0.6	B2	4.7 ± 0.6	0.0081	0.0162
A3		B3			
A4	2.7 ± 0.7	B4	5.9 ± 0.8	0.0005	0.0015
A5		B5			
A6	3.0 ± 0.7	B6	6.7 ± 1.1	<.0001	0.0004

A1 = Protocol A at Time Point 1. Values are means ± SE, units in %. Data was not sampled at B3 and B5 due to the subjects exercising. BH = Bonferroni-Holm corrected p-value. Red indicates statistically significant p-values and/or BH p-values.

### **Specific Aim 3:**

**To determine how radial position along a centrifuge arm and the resultant blood redistribution affect heart rate during centrifugation. The following hypothesis will be tested:**

**Hypothesis 3: Heart rates will be greater for long radius without exercise (LRC-) than for short radius without exercise (SRC-).**

Heart rate responses for LRC- nearly mirrored that of SRC- with an approximate +7 beat per minute baseline shift (Figure 7.9). Figure 5.3 previously shown defines the Time Point nomenclature used in the heart rate plots and tables. The heart rate trend oscillated in response to G-level with elevated heart rates at 1.25G compared to 1G (not statistically tested). The control period (Time Point 1) was included to gauge the response induced by the familiarization spin in relation to the post-familiarization control period (Time Point 2).



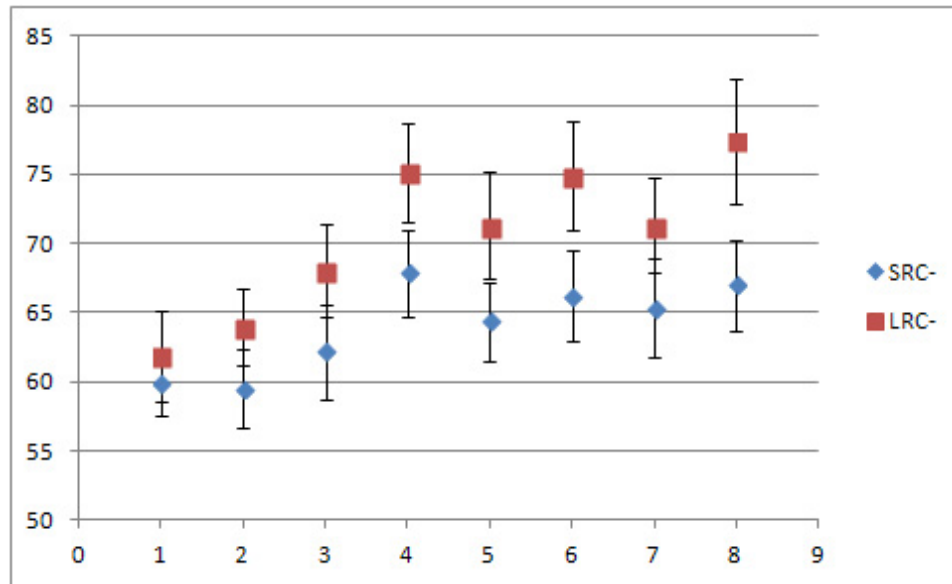


Figure 7.9: Heart rates SRC- versus LRC-. Values are means  $\pm$  SE.  
 Abscissa: Time Point (1 thru 8). Ordinate: Beats Per Minute.

The main effect of protocol was not significant at  $p = 0.15$ . Although the trend was present that LRC- had elevated heart rates at Time Points 3 through 8, none were statistically larger than SRC- (Table 7.9).

Table 7.9: Heart rates SRC- (Protocol A) versus LRC- (Protocol C) statistical summary.

	SRC-		LRC-	p-value	BH p-value
A1	60 ± 2	C1	62 ± 3	0.51	0.51
A2	60 ± 3	C2	64 ± 3	0.27	0.54
A3	62 ± 3	C3	68 ± 3	0.23	0.70
A4	68 ± 3	C4	75 ± 4	0.13	0.79
A5	64 ± 3	C5	71 ± 4	0.15	0.74
A6	66 ± 3	C6	75 ± 4	0.08	0.58
A7	65 ± 4	C7	71 ± 3	0.21	0.83
A8	67 ± 3	C8	77 ± 5	0.04	0.35

A1 = Protocol A at Time Point 1. Values are means ± SE, units in bpm. BH = Bonferroni-Holm corrected p-value. **Red** indicates statistically significant p-values and/or BH p-values.

#### Specific Aim 4:

To determine how lower limb exercise and the resultant blood redistribution affect heart rate during centrifugation. The following hypothesis will be tested:

**Hypothesis 4: Heart rates will be greater for short radius with exercise (SRC+) than for short radius without exercise (SRC-).**

Heart rates for SRC+ were by and far different from SRC- (Figure 7.10). The heart rates for SRC+ did not respond to G-level, but instead to the repetitive bouts of exercise.

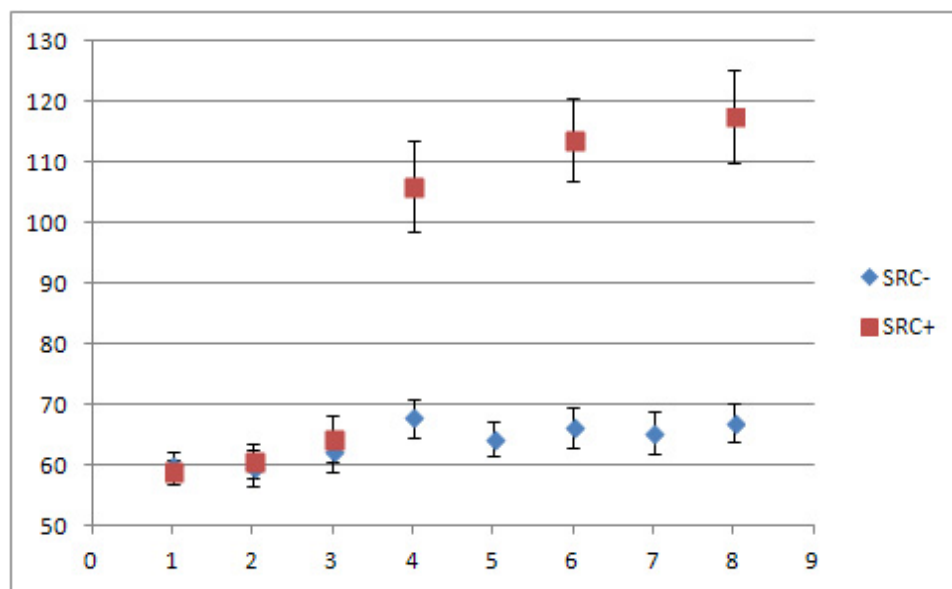


Figure 7.10: Heart rates SRC- versus SRC+. Values are means  $\pm$  SE.

Abscissa: Time Point (1 thru 8). Ordinate: Beats Per Minute.

The main effect of protocol was significant at  $p = 0.0014$ . The heart rates were statistically different at Time Points 4, 6, and 8 (Table 7.10) as expected from looking at Figure 7.10. The heart rates were not statistically different at Time Points 1, 2, and 3 as anticipated because both protocols provided the same stimulus at those Time Points.

Table 7.10: Heart rates SRC- (Protocol A) versus SRC+ (Protocol B) statistical summary.

	SRC-		SRC+	p-value	BH p-value
A1	60 ± 2	B1	59 ± 2	0.5363	0.9999
A2	60 ± 3	B2	61 ± 3	0.8347	0.9999
A3	62 ± 3	B3	64 ± 4	0.9672	0.9999
A4	68 ± 3	B4	106 ± 7	<0.0001	0.0006
A5		B5			
A6	66 ± 3	B6	114 ± 7	<0.0001	0.0005
A7		B7			
A8	67 ± 3	B8	118 ± 8	<0.0001	0.0004

A1 = Protocol A at Time Point 1. Values are means ± SE, units in bpm. Data was not sampled at B5 and B7 due to the subjects exercising. BH = Bonferroni-Holm corrected p-value. Red indicates statistically significant p-values and/or BH p-values.

## Chapter Eight: Discussion

### Specific Aim 1:

To determine how radial position along a centrifuge arm affects blood redistribution during centrifugation. The following hypothesis will be tested:

**Hypothesis 1: Net fluid shift from the thorax will be greater for long radius without exercise (LRC-) than for short radius without exercise (SRC-).**

#### **Thorax**

As hypothesized, the fluid shift from the thorax was larger for LRC- than SRC-. This conclusion is supported by the -10 to -12% changes in volume of the thorax measured for LRC-; opposed to the -6 to -10% changes for SRC- (Figure 7.1). Summarized previously in Table 7.1, LRC- was statistically greater than SRC- at each Time Point (1 through 6). The fluid loss (likely loss of venous blood volume) for LRC- presented an increased challenge to cardiovascular regulation as was anticipated with the larger net acceleration forces due to increased radius (Figure 4.5).

#### **Abdomen**

The fluid shift into the abdomen trended larger for LRC- than SRC-; however, this apparent difference was not statistically significant as summarized previously in Table 7.2. Shown in Figure 7.2, the fluid gain for LRC- measured

from +7 to +8%, opposed to around +5% for SRC-. From the trend, it appears as though the increased fluid loss from the thorax shifted to the abdominal region accounting for most, if not all of the increased fluid mass lost from the thorax during LRC-.

## Upper Leg

Similar to SRC-, LRC- showed -1 to -2% changes as depicted previously in Figure 7.3. As expected from viewing Figure 7.3, Table 7.3 showed no statistical difference. The data show that fluid (blood) was lost in the upper leg, a finding that was not anticipated. Shown previously (Figure 6.13) the upper leg gained fluid during upright tilt. Given the data at hand, differential effects of centrifugation and upright tilt on upper leg blood volume exist. A study published by Taneja and colleagues presented differential effects of lower body negative pressure (LBNP) and upright tilt on splanchnic blood volume (Taneja et al. 2007). They found that splanchnic blood volume decreased with lower body negative pressure and increased with upright tilt. They attributed the difference to the effects of gravity present with the upright tilt and lacking with the LBNP. In the present study SRC- and LRC- provided artificial gravity via centrifugation; a completely different modality than Earth gravity via upright tilt. The upper leg lost fluid likely due to venous emptying, which could have been caused by vasoconstriction. Perhaps the centrifuge rotation and centripetal acceleration triggered neural mechanisms to induce vasoconstriction in the upper leg segment. The differential effects in the present study could also be explained by the difference in net gravito-inertial forces experienced between the upright tilt and centrifuge. A 70° upright tilt yields a constant  $1G_{ZX}$  vector at 20° along the length of the body. Compared to the net gravito-inertial forces experienced on the centrifuge (Figure 4.5) during SRC- and LRC-, the upright tilt yielded smaller  $G_{ZX}$  vectors but at a much more acute angle in relation to the  $G_Z$  axis. The net

gravito-inertial forces were typically at a 45° angle during SRC- and LRC-. Taneja and colleagues (2007) reported fluid gain in the pelvic region (upper leg in present study) during 20°, 40°, and 70° upright tilts. Thus it is more likely that the mode of gravity was responsible for the differential upper leg effects in the present study.

## **Lower Leg**

Similar to SRC-, LRC- showed +2 to +3% changes as depicted previously in Figure 7.4. As expected from viewing Figure 7.4, Table 7.4 showed no statistical difference. LRC- provided little additional stimulus over SRC- in terms of the lower leg. Both SRC- and LRC- were normalized to provide 1G<sub>z</sub> at the foot, thus the acceleration stimuli were similar in the lower leg.

## **Summary**

Hypothesis 1 was found to be true. However, the lack of statistical significance for the abdomen does not allow for concrete accounting of the additional loss from the thorax. LRC- presented a greater challenge to the cardiovascular system as shown in the thoracic fluid shifts. However based on the trend, the additional fluid loss from the thorax was simply distributed to the abdomen which may not be ideal for an artificial gravity protocol. Blood pooling in the abdominal region has been linked to orthostatic intolerance (Montgomery et al. 1977, Buckey et al. 1996, White et al. 1996, Arbeille et al. 2008). No difference in fluid shifts between SRC- and LRC- was found for the upper and lower leg segments, but fluid was lost from the upper leg during centrifugation and gained during upright tilt.

A long radius centrifuge such as tested with LRC- is not likely to fly in space due to physical spacecraft space (cubic feet) and monetary reasons; whereas a small radius centrifuge could be practically implemented, such as proposed with the NASA Ames Human Powered Centrifuge (Greenleaf et al. 1996). Thus, the fluid shift results from comparing short radius versus long radius are perhaps fortunate when one thinks about operational implementation during spaceflight.



## **Specific Aim 2:**

**To determine how lower limb exercise affects blood redistribution during centrifugation. The following hypothesis will be tested:**

**Hypothesis 2: Net fluid shift from the thorax will be greater for short radius with exercise (SRC+) than for short radius without exercise (SRC-).**

### **Thorax**

As hypothesized, the fluid shift from the thorax was larger for SRC+ than SRC-. This conclusion is supported by the -12 to -14% changes in volume of the thorax measured for SRC+; opposed to the -6 to -10% changes for SRC- (Figure 7.5). Summarized previously in Table 7.5, SRC+ was statistically greater than SRC- at all three of the post-exercise Time Points. The additional fluid loss (likely loss of venous blood volume) for SRC+ presented an increased challenge to cardiovascular regulation as expected with this unique combination of centrifugation plus exercise. The uniqueness in SRC+ lies in the fact that the subjects exercised, stopped and resumed the legs extended posture, and then were exposed to a higher  $G_z$  level. It was during these “static” legs extended portions that bio-electrical impedance measurements were analyzed, not during the actual “dynamic” exercise leg pedaling periods. Bio-electrical impedance signals are impacted by muscle activity and thus an accurate value likely cannot be acquired while the subjects are voluntarily moving, particularly during leg pedaling.

## Abdomen

The resultant fluid shift response in the abdomen during SRC+ is potentially the most important finding from this investigation. Shown previously in Figure 7.6, the fluid gain for SRC- was relatively constant around +5%; whereas with SRC+ the fluid gain started around +5% but after the exercise commenced the fluid gain eventually reduced to +2%. Summarized in Table 7.6, Time Point 1 was not statistically different as expected, but after subsequent bouts of exercise the fluid shift during SRC+ was significantly less than the fluid shifted during SRC- at Time Points 4 and 6. Rather than blood “pooling” in the abdominal region, by adding uniquely-timed exercise to centrifugation, blood was essentially “mobilized” to other body segments, namely the upper and lower leg as described below. Except for the capillaries, all splanchnic blood vessels receive sympathetic innervation (Boron and Boulpaep 2011). A major value of sympathetic vasoconstriction in the gut is that it allows shutoff of gastrointestinal and other splanchnic blood flow for short periods of time during heavy exercise, when the skeletal muscle and heart need increased flow (Hall 2011). Vasoconstriction elicited by sympathetic nerve activity can reduce blood flow to less than ~25% of resting values (Boron and Boulpaep 2011). Sympathetic stimulation also causes strong vasoconstriction of the large-volume intestinal and mesenteric veins (Hall 2011). This decreases the volume of these veins, thereby displacing large amounts of blood into other parts of the circulation (Hall 2011).

## Upper Leg

The fluid shift response in the upper leg is as important as the finding in the abdomen; however, the upper leg response was anticipated due to the underlying nature of exercise and the unique design of the SRC+ protocol. Shown previously in Figure 7.7, SRC+ provided fluid increases of +1, +3, and

+5% after bouts of exercise; as opposed to SRC- which showed a -2% flat response. Summarized in Table 7.7, Time Point 1 was not statistically different between the protocols as expected, but Protocol B was significantly different at Time Points 2, 4, and 6. Exercise provided the stimulus needed to increase blood volume in the upper leg as anticipated by the design of SRC+. During rest, some muscle capillaries have little or no flowing blood; but during strenuous exercise, all the capillaries open (Hall 2011). During extreme exercise in the well-conditioned athlete, blood flow through skeletal muscle can increase 25- to 50-fold over resting values (Hall 2011). As shown in the calf, blood flow increases and decreases with each muscle contraction during rhythmical muscular exercise (Barcroft and Dornhorst 1949, Hall 2011). The cause of the lower flow during the muscle contraction phase of exercise is compression of the blood vessels by the contracted muscle (Hall 2011). At the end of the contractions (exercise), the blood flow remains very high for a few seconds but then returns toward normal during the next few minutes (Barcroft and Dornhorst 1949, Hall 2011).

The integration of exercise and centrifugation would most likely be necessary in order to achieve the same result in the upper leg during spaceflight while in microgravity. Measurements were made post-exercise in this study and the blood likely pooled in the upper leg due to the “gravitational” forces provided by the centrifuge. One pitfall of this study was the lack of an exercise control without the centrifuge spinning so some speculation exists; however, during any practical implementation in spaceflight both centrifuge rotation and exercise will most likely be needed simultaneously.

## **Lower Leg**

Shown in Figure 7.8, SRC+ provided +5 to +7% changes in lower leg volume as result of the exercise; as opposed to +2 to +3% responses during

SRC-. As summarized in Table 7.8, fluid shifts were not different at Time Point 1, as expected, but fluid shifts during SRC+ were significantly larger than fluid shifts during SRC- at Time Points 2, 4, and 6. Similar to the upper leg, exercise resulted in increased blood volume in the lower leg.

## Summary

Hypothesis 2 was found to be true. Centrifugation plus specifically-timed exercise provided a notable response compared to centrifugation alone. Exercise significantly affected each of the four body segments. More fluid loss occurred in the thorax which provided a challenging stimulus to invoke cardiovascular regulation. In spite of increased fluid loss from the thorax, less blood “pooled” in the abdominal region and instead was “mobilized” to the upper and lower leg.

### **Specific Aim 3:**

To determine how radial position along a centrifuge arm and the resultant blood redistribution affect heart rate during centrifugation. The following hypothesis will be tested:

**Hypothesis 3: Heart rates will be greater for long radius without exercise (LRC-) than for short radius without exercise (SRC-).**

As hypothesized, the heart rates for LRC- trended greater than SRC- (Figure 7.9); albeit, differences were not statistically significant (Table 7.9). Overall, LRC- averaged around 8 beats per minute higher than SRC-; with the range being 6 to 10 beats higher at the various Time Points. The modest heart rate increases for LRC- were tied to the -2 to -3%, on average, greater fluid shift from the thorax during LRC- versus SRC-.

#### **Specific Aim 4:**

To determine how lower limb exercise and the resultant blood redistribution affect heart rate during centrifugation. The following hypothesis will be tested:

**Hypothesis 4: Heart rates will be greater for short radius with exercise (SRC+) than for short radius without exercise (SRC-).**

As hypothesized, heart rates for SRC+ were significantly greater than heart rates for SRC- (Figure 7.10) and (Table 7.10). Overall, SRC+ averaged around 46 beats per minute higher than SRC-; with the range being 38 to 51 beats higher at Time Points 4, 6, and 8. A protocol dedicated to exercise without the centrifuge spinning would have to be conducted to fully decouple the exercise response from the acceleration response provided during SRC+. This new dedicated protocol would be a SRC+ repeat, except with the centrifuge not spinning. Other than this, the primary conclusion is the difference in heart rate was due to the exercise.

## **Chapter Nine: Noteworthy Findings**

### **Simultaneous Plethysmography Measurements**

Many studies have used strain-gauge plethysmography around the calf of the leg to measure fluid shifts in response to orthostatic stress; whereas, limited studies are available in which fluid shift was measured in multiple segments simultaneously with electrical impedance as is the case with the current study. Strain-gauge plethysmography of the calf is rather easy to employ and thus its prominence amongst research studies. The lower leg (calf) volume is small in comparison to the upper leg or the abdomen and thus the fluid shift potential is limited. This document provides data showing that the upper leg and lower leg can act independently of one another, meaning that one segment can lose fluid volume (upper leg) while the other gains fluid volume (lower leg). A recent study targeted the calf and its role in orthostatic hypotension with autonomic failure but found no correlation between the degree of orthostatic hypotension and the orthostatic calf volume change (Thijs et al. 2010). Data presented in this document support the argument that a more complete view of body segment fluid distribution in response to orthostatic stress should be made.

### **Artificial Gravity Protocol Design**

This document proposed that a properly designed artificial gravity protocol for use during human spaceflight will imitate the effects of the gravitational environment of Earth (Clement et al. 2007, Paloski et al. 2009) and will yield a net shift of blood from the thorax to the upper leg and lower leg without detrimental accumulation of blood in the abdomen. Pooling of blood in the abdomen likely is undesirable for optimal maintenance of blood pressure

homeostasis during gravitational challenges (Montgomery et al. 1977, Buckey et al. 1996, White et al. 1996, Arbeille P et al. 2008). Smit et al. (2004) showed that abdominal binders were effective in reducing orthostatic hypotension in patients with autonomic failure. Denq et al. (1997) and Tanaka et al. (1997) previously published similar findings to that of Smit et al. (2004). Diedrich and Biaggioni's sample bio-electrical impedance data from a tilt test showed that 75% of the fluid that shifted from the thorax went to the abdomen (Diedrich and Biaggioni 2004). Diedrich and Biaggioni concluded that the abdomen was by far the greatest reservoir of orthostatic fluid shifts and was where most of the pooling was occurring.

The importance of the abdominal region / splanchnic circulation and its role in orthostatic intolerance has not gone unnoticed by spaceflight researchers at NASA Johnson Space Center. A recent publication shows that abdomen-high elastic gradient compression garments are promising as a countermeasure against post-spaceflight orthostatic intolerance (Stenger et al. 2013). Including the abdominal region is an evolution from their prior work showing that thigh-high only garments were effective in preventing post-spaceflight symptoms of orthostatic intolerance after a Space Shuttle mission (Stenger et al. 2010). They recognized studies suggesting that abdominal compression improves the efficacy of compression garments (Tanaka et al. 1997, Denq et al. 1997, Smit et al. 2004).

In the present centrifuge study, specifically-timed exercise combined with centrifugation (SRC+) provided a unique stimulus in which fluid was "mobilized" from the abdomen to the upper and lower leg. The fluid shift profile during SRC+ mirrored what has been proposed in this document as desirable: fluid loss from the thorax, fluid gain in the upper and lower leg, and mitigation of gain in the abdomen. It is anticipated that a properly designed protocol performed in microgravity will maintain the peripheral vasculature's abilities at a level sufficient to facilitate venous return to the heart during orthostatic challenges upon return to a gravitational environment such as Earth. Prior work has shown that an



inability to increased total peripheral resistance is normally seen during orthostatic stress after spaceflight (Buckey et al. 1996, Fritsch-Yelle et al. 1996, Waters et al. 2002).

### **Underlying Mechanism(s) Explaining Increased Orthostatic Tolerance**

The exercise fluid shift profile presented in this document is applicable to not only artificial gravity protocol design but also proposes a mechanistic reason as to why certain artificial gravity protocols are more effective than others in increasing orthostatic tolerance. Research has shown that centrifugation powered by cycle exercise was effective in increasing orthostatic tolerance in ambulatory men and women (Stenger et al. 2007). They found that men received more benefit than women and that active training (exercise) was more beneficial than passive training (non-exercise). They concluded that more research was needed to determine precise mechanisms of improvement in order to elucidate the ideal artificial gravity training regimen to prevent orthostatic intolerance after spaceflight for both men and women. The research findings presented in this document are a key piece of the puzzle in determining mechanisms that underlie the orthostatic tolerance improvement. During SRC- (passive), the abdomen acted as a reservoir for blood “pooling”. During SRC+ (active), the fluid shift to the abdomen was mitigated and “mobilized” to the upper and lower leg. The exercise during SRC+ was specifically-timed to induce fluid shift into the upper and lower leg; whereas, in the Stenger et al. (2007) study the subjects who were active exercised continuously throughout the protocol. It cannot be concluded with the data at hand, but it is reasonable to believe that fluid would not “pool” in the abdomen while active leg muscle beds were vasodilated, as was the case with the Stenger et al. (2007) study. The results presented in this document support the hypothesis that one underlying reason for increased orthostatic tolerance from centrifugation protocols with lower limb

exercise is the fluid shift away from the abdomen into the upper and lower leg. In the Stenger et al. (2007) study, active women improved tolerance while passive women did not. Women have different internal organ structure (mainly reproductive) in their splanchnic region compared to men. Pooling of fluid in this region has been reported as one of the major reasons why women are less tolerant to lower body negative pressure stress than men (Montgomery et al. 1977, White et al. 1996). Perhaps centrifugation protocols with lower limb exercise train the vasculature to mitigate pooling in the abdominal region and is one mechanism by which improved orthostatic tolerance occurs.

A recent study conducted at NASA Johnson Space Center (JSC) testing the efficacy of artificial gravity as a multi-system countermeasure to bed-rest induced (spaceflight analog) deconditioning yielded mixed results. It was concluded that artificial gravity training mitigated some aspects of bed rest-induced cardiovascular deconditioning in men, namely orthostatic intolerance (Stenger et al. 2012). The NASA JSC study's artificial gravity protocol was similar to that of SRC- in the present study; however, with some differences. The JSC study involved subjects "standing" on a force plate as opposed to "sitting" on a bicycle seat during centrifugation,  $1G_z$  was normalized at the heart as opposed to the foot level, and the subjects did not exercise aside from some calf raises performed to prevent presyncopal symptoms. As shown in this document, a static-type protocol without lower limb exercise did not result in a favorable distribution of body segment fluid volumes. Perhaps had the JSC study included lower limb exercise and induced what is believed to be a more appropriate fluid shift, the artificial gravity training would have been more effective against the bed-rest induced deconditioning.

## **Chapter Ten: Study Limitations and Recommendations for Future Work**

### **Supine Exercise Response**

In the study performed for this document, only supine exercise with centrifugation was available; a stand-alone protocol with supine exercise without centrifugation was not performed. The need exists to measure fluid shifts and heart rate responses for exercise on a centrifuge without it spinning and with it spinning to truly understand the nature of how exercise and acceleration forces integrate. Of particular interest would be to determine fluid shift responses of the upper leg and the abdomen when repeated bouts of exercise are performed in the supine position without centrifuge acceleration forces. What is the supine exercise response without the centrifuge acceleration forces? This information is needed in order to optimize exercise artificial gravity protocols intended for use during spaceflight.

### **Upright Tilt Fluid Shift Profile of Subjects Pre- and Post-AG Training**

To test whether the fluid shift into the abdomen is mitigated during gravitational stress as result of active (with lower limb exercise) artificial gravity training, a study similar to Stenger et al. (2007) would have to be performed using bio-electrical impedance to measure the fluid shift profile pre- and post-AG training. As in that study, it would be beneficial to use both men and women subjects.

## Significance of Leg Position on Fluid Shift Profile

With the data available, it was not possible to perform a thorough analysis comparing legs extended with feet unsupported, feet on the plates, and feet up on bicycle pedals. The data presented in this document include only the legs extended with feet unsupported position. The feet on the plates and feet up on bicycle pedals are not included in the current analysis. Leg position could likely be an important variable when working toward optimizing protocol designs. Of particular interest is the impact of feet up on bicycle pedals because this position changes the orientation of the hydrostatic column of blood from the heart to the feet. The hydrostatic column is shortened in the  $G_z$  axis because of the bent knee moving the upper and lower leg segment along the  $G_x$  axis.

## APPENDICES

### Appendix A: Butterworth Low-Pass Filter MATLAB Code

#### **%Assign Names to Data Channels**

```
Thorax_Ro = A(1:end,12);  
Abdomen_Ro = A(1:end,16);  
UpperLeg_Ro = A(1:end,20);  
LowerLeg_Ro = A(1:end,24);  
GFoot = A(1:end,5);
```

#### **%Known Sampling Frequency and Calculated Nyquist Frequency**

```
fs = 1000;  
Ny = fs/2;
```

#### **%Butterworth Low-Pass Filter for Segmental Impedance Ro Fluid Shifts**

```
fcSegImpRo = 0.6; %cutoff frequency  
WnSegImpRo = fcSegImpRo/Ny; %normalized cutoff frequency  
orderSegImpRo = 5; %order of filter  
[bSegImpRo,aSegImpRo] = butter(orderSegImpRo,WnSegImpRo,'low'); %Butterworth  
LPF design  
low_Thorax_Ro = filtfilt(bSegImpRo,aSegImpRo,Thorax_Ro); %zero-phase filtered  
data  
low_Abdomen_Ro = filtfilt(bSegImpRo,aSegImpRo,Abdomen_Ro); %zero-phase  
filtered data  
low_UpperLeg_Ro = filtfilt(bSegImpRo,aSegImpRo,UpperLeg_Ro); %zero-phase  
filtered data  
low_LowerLeg_Ro = filtfilt(bSegImpRo,aSegImpRo,LowerLeg_Ro); %zero-phase  
filtered data  
low_GFoot = filtfilt(bSegImpRo,aSegImpRo,GFoot); %zero-phase filtered data
```

## Appendix B: Electrical Impedance Plethysmography

### Background

The bio-electrical impedance method offers all the advantages of the indirect techniques used in the biomedical sciences, the most being that in many applications the integument need not be penetrated to make the measurement (Geddes and Baker 1989). However, the impedance method is subject to limitations inherent in many indirect techniques (Geddes and Baker 1989). Frequently the signal is obtained at a distance from the phenomenon, thus resolution is compromised, and the signal is often difficult to calibrate in true physiological terms (Geddes and Baker 1989). Uncalibratable signals that directly reflect a physiological event can have considerable value for monitoring changes under a variety of experimentally controlled conditions (Geddes and Baker 1989). Uncalibrated tracking signals have value in time-domain studies (Geddes and Baker 1989).

Impedance plethysmography, the electrical conductivity method, gives a physical measure of the ionic conduction of a given body segment in contrast with electronic conduction characteristic of metallic substances (Nyboer et al. 1950). Transient and static values of electrical conductivity are associated, respectively, with dynamic and balanced conditions of arteriovenous blood volume differences within a given segment (Nyboer et al. 1950). If the blood pools indefinitely or transiently within a segment, its resistivity will be added in some manner to the resistivity of the segment (Nyboer et al. 1950). Continuous records of electrical conductivity of a body segment trace the course of a blood volume pulse and measure its magnitude by virtue of the number and mobility of ions (Nyboer et al. 1950). The various functions of the peripheral circulation which may be defined by impedance measures are: pulse volume, pulse form, pulse velocity, the rate of change of pulse volume, as well as blood pooling and emptying – particularly of the venous reservoirs (Nyboer et al. 1950).

Impedance plethysmography measures changes in the flow of an electrical current through a body segment that occur with changes in the fluid-volume content of the segment (Montgomery et al. 1993). Basal impedance of a body segment is determined by the relative content of the various conductive tissues within the segment (Montgomery et al. 1993). However, since blood is more conductive and mobile than bone, muscle or skin, transient changes in segmental impedance during short-term experiment protocols may be attributed primarily to blood pooling and circulatory changes within the intravascular space of the segment (Montgomery et al. 1993). Since blood is a conductive electrolyte, the impedance of a given body segment is dependent upon the amount of blood contained within the segment at any given point in time (Montgomery et al. 1993). As blood enters the segment, during each cardiac cycle or as a result of fluid redistribution, its impedance decreases (Montgomery et al. 1993). Conversely, as blood flows out of the segment its impedance increases (Montgomery et al. 1993).

The concept that the volume of a substance is a direct function of its electrical conductivity is taught in elementary physics of conductors in relation to electronic conduction (Nyboer et al. 1950). There is no justification for believing that it does not apply to ionic conductors, such as blood (Nyboer et al. 1950). If the blood does not alter too rapidly in its electrolyte to non-electrolyte ratio, its conductivity should justifiably enter into volume determination as it is directly proportional to the measure of segmental volume (Nyboer et al. 1950).

### **Mathematical Expression for Volume of Electrical Conductors**

The resistance ( $R$ ) in ohms of a length of homogeneous cylindrical electronic conductive material of uniform cross-sectional area is proportional to its length ( $L$ ) in centimeters and inversely proportional to its cross-sectional area

(A) in square centimeters (Nyboer 1970, Montgomery et al. 2011). The resistance of the conductor is given by

$$R = \rho L / A \quad \text{Equation B1}$$

where  $\rho$  is the electrical resistivity of the conductive medium in ohm-cm when the length and cross-sectional area are each equal to one unit (Nyboer 1970, Montgomery et al. 2011). The resistivity factor expresses the resistivity of 1 cm<sup>3</sup> of the material being measured. Multiplying Equation B1 by L / L (Nyboer 1970, Montgomery et al. 2011) provides

$$R = \rho L / A * L / L$$

where  $V = A \cdot L$ , the volume of the conductive medium, thus yielding

$$R = \rho * L^2 / V$$

Transposing the V and R (Nyboer 1970, Montgomery et al. 2011) provides

$$V = \rho L^2 / R \quad \text{Equation B2}$$

Thus if the length, resistivity, and resistance of a conductor are known or are measurable one should be able to calculate the volume of such an electrical conductor. This basic physical principle of electronic volume determination will be applied to the calculation of the unknown volume of an ionic conductor (Nyboer 1970). Equation B2 forms the basis of impedance plethysmographic measurement of segmental volumes within the human body (Nyboer et al. 1950, Nyboer 1970, Diedrich and Biaggioni 2004, Montgomery et al. 2011).



## Derivation of Impedance Volume Percent Change

Volume of a conductor or body segment (Equation B2):

$$V = \rho L^2 / R$$

Volume of body segment at post-fam (PF) and at a G level (G):

$$V_{PF} = \rho L^2 / R_{PF} \quad \text{and} \quad V_G = \rho L^2 / R_G$$

Percent change of delta volume:

$$\Delta V \% \text{ change} = (V_G - V_{PF} / V_{PF}) * 100$$

$$\Delta V \% \text{ change} = ((\rho L^2 / R_G - \rho L^2 / R_{PF}) / \rho L^2 / R_{PF}) * 100$$

Assuming  $\rho$  is relatively constant:

$$\Delta V \% \text{ change} = ((1/R_G - 1/R_{PF}) / 1/R_{PF}) * 100$$

$$\Delta V \% \text{ change} = ((R_{PF} - R_G / R_G R_{PF}) / (1/R_{PF})) * 100$$

Equation B3, expression used for percent change of volume:

$$\Delta V \% \text{ change} = (R_{PF} - R_G / R_G) * 100 \quad \text{Equation B3}$$

## REFERENCES

**Arbeille P, Kerbeci P, Mattar L, Shoemaker JK, Hughson R.** Insufficient flow reduction during LBNP in both splanchnic and lower limb area is associated with orthostatic intolerance after bedrest. *Am J Physiol Heart Circ Physiol* 295: H1846-54, 2008.

**Barcroft H, Dornhorst AC.** The blood flow through the human calf during rhythmic exercise. *J Physiol* 109: 402-411, 1949.

**Boron WF, Boulpaep EL.** Medical Physiology (Second Edition). Philadelphia: Saunders Elsevier, 2011.

**Buckey JC.** Preparing for Mars: The physiologic and medical challenges. *Eur J Med Res* 4: 353-356, 1999.

**Buckey JC.** Space Physiology. New York: Oxford University Press, 2006.

**Buckey JC, Lane LD, Levine BD, Watenpaugh DE, Wright SJ, Moore WE, Gaffney FA, Blomqvist CG.** Orthostatic intolerance after spaceflight. *J Appl Physiol* 81(1): 7-18, 1996.

**Bukley A, Paloski W, Clement G.** Artificial Gravity. Chapter 2: Physics of artificial gravity. New York: Springer Science+Business Media, 2007.

**Clement G, Pavy-Le Traon A.** Centrifugation as a countermeasure during actual and simulated microgravity: a review. *Eur J Appl Physiol* 92: 235-248, 2004.

**Clement G, Bukley A, Paloski W.** Artificial Gravity. Chapter 1: The gravity of the situation. New York: Springer Science+Business Media, 2007.

**Denq JC, Opfer-Gehrking TL, Giuliani M, Felten J, Convertino VA, Low PA.** Efficacy of compression of different capacitance beds in the amelioration of orthostatic hypotension. *Clin Auton Res* 7: 321-6, 1997.

**Diedrich A, Biaggioni I.** Segmental orthostatic fluid shifts. *Clin Auton Res* 14: 146-147, 2004.

**Evans JM, Stenger MB, Moore FB, Hinghofer-Szalkay H, Rossler A, Patwardhan AR, Brown DR, Ziegler MG, Knapp CF.** Centrifuge training increases presyncope orthostatic tolerance in ambulatory men. *Aviat Space Env Med* 75(10): 850-8, 2004.

**Fritsch-Yelle JM, Charles JB, Jones MM, Beightol LA, Eckberg DL.** Spaceflight alters autonomic regulation of arterial pressure in humans. *J Appl Physiol* 77: 1776-1783, 1994.

**Fritsch-Yelle JM, Whitson PA, Bondar RL, Brown TE.** Subnormal norepinephrine release relates to presyncope in astronauts after spaceflight. *J Appl Physiol* 81: 2134-41, 1996.

**Geddes LA, Baker LE.** Principles Of Applied Biomedical Instrumentation (Third Edition). New York: John Wiley & Sons, 1989.

**Greenleaf JE, Gundo DP, Watenpaugh DE, Mulenburg GM, Marchman N, Looft-Wilson R, Hargens AR.** Cycle-powered short radius (1.9M) centrifuge: exercise vs. passive acceleration. *J Gravit Physiol* 3(2): 61-62, 1996.

**Hall JE.** Guyton and Hall Textbook of Medical Physiology (Twelfth Edition). Philadelphia: Saunders Elsevier, 2011.

**Hastreiter D, Young LR.** Effects of a gravity gradient on human cardiovascular responses. *J Gravit Physiol* 4(2): 23-6, 1997.

**Levine BD, Lane LD, Watenpaugh DE, Gaffney FA, Buckey JC, Blomqvist CG.** Maximal exercise performance after adaptation to microgravity. *J Appl Physiol* 81: 686-694, 1996.

**Meck JV, Reyes CJ, Perez SA, Goldberger AL, Ziegler MG.** Marked exacerbation of orthostatic intolerance after long- vs. short-duration spaceflight in veteran astronauts. *Psychosom Med* 63: 865-73, 2001.

**Montgomery LD, Kirk PJ, Payne PA, Gerber RL, Newton SD, Williams BA.** Cardiovascular responses of men and women to lower body negative pressure. *Aviat Space Env Med* 48: 138-145, 1977.

**Montgomery LD, Parmet AJ, Booher CR.** Body volume changes during simulated microgravity: Auditory changes, segmental fluid redistribution, and regional hemodynamics. *Ann Biomed Eng* 21(4): 417-433, 1993.

**Montgomery LD, Dietrich MS, Armer JM, Stewart BR, Ridner SH.** Segmental Blood Flow and Hemodynamic State of Lymphedematous and Nonlymphedematous Arms. *Lymphat Res Biol* 9(1): 31-42, 2011.

**Nyboer J, Kreider MM, Hannapel L.** Electrical impedance plethysmography: A physical and physiologic approach to peripheral vascular study. *Circulation* 2: 811-821, 1950.

**Nyboer J.** Electrical Impedance Plethysmography (Second Edition). Springfield: Thomas Books, 1970.

**Paloski WH, Young L, Fuller C, Jarchow T.** Artificial Gravity Research To Enable Human Space Exploration. International Academy of Astronautics, 2009.

**Rowell LB.** Human Cardiovascular Control. New York: Oxford University Press, 1993.

**Smit AA, Wieling W, Fujimura J, Denq JC, Opfer-Gehrking TL, Akarriou M, Karemaker JM, Low PA.** Use of lower abdominal compression to combat orthostatic hypotension in patients with autonomic dysfunction. *Clin Auton Res* 14(3): 167-75, 2004.

**Stenger MB.** Human cardiovascular responses to artificial gravity training. Ph.D. Dissertation Graduate School University of Kentucky, 2005.

**Stenger MB, Evans JM, Patwardhan AR, Moore FB, Hinghofer-Szalkay H, Rossler A, Ziegler MG, Knapp CF.** Artificial gravity training improves orthostatic tolerance in ambulatory men and women. *Acta Astronautica* 60: 267-272, 2007.

**Stenger MB, Brown AK, Lee S, Locke JP, Platts SH.** Gradient compression garments as a countermeasure to post-spaceflight orthostatic intolerance. *Aviat Space Environ Med* 81: 883-7, 2010.

**Stenger MB, Evans JM, Knapp CF, Lee S, Phillips TR, Perez SA, Moore AD, Paloski WH, Platts SH.** Artificial gravity training reduces bed rest-induced cardiovascular deconditioning. *Eur J Appl Physiol* 112: 605-616, 2012.

**Stenger MB, Lee S, Westby CM, Ribeiro LC, Phillips TR, Martin DS, Platts SH.** Abdomen-high elastic gradient compression garments during post-spaceflight stand tests. *Aviat Space Environ Med* 84: 459-66, 2013.

**Tanaka H, Yamaguchi H, Tamai H.** Treatment of orthostatic intolerance with inflatable abdominal band. *Lancet* 349:175, 1997.

**Taneja I, Moran C, Medow MS, Glover JL, Montgomery LD, Stewart JM.** Differential effects of lower body negative pressure and upright tilt on splanchnic blood volume. *Am J Physiol Heart Circ Physiol* 292: H1420-26, 2007.

**Thijs RD, Kamper AM, van Dijk AD, van Dijk JG.** Are the orthostatic fluid shifts to the calves augmented in autonomic failure? *Clin Auton Res* 20(1): 19-25, 2010.

**Vernikos J.** Artificial gravity intermittent centrifugation as a space flight countermeasure. *J Gravit Physiol* 4(2): 13-16, 1997.

**Waters WW, Ziegler MG, Meck JV.** Postspaceflight orthostatic hypotension occurs mostly in women and is predicted by low vascular resistance. *J Appl Physiol* 92: 586-94, 2002.

**White DD, Montgomery LD.** Pelvic blood pooling of men and women during lower body negative pressure. *Aviat Space Environ Med* 67: 555-559, 1996.

**White RJ, Averner M.** Humans in space. *Nature* 409: 1115-1118, 2001.

## VITA

Mark Steven Howarth

### Education

B.S. Aerospace Engineering, Minor Mathematics  
Embry-Riddle Aeronautical University

### Professional Positions Held

2013- Mechanical Hardware Engineer – Lexmark  
2010-12 Research, Development, and Reliability Engineer – Adecco  
2008-09 Design Engineer – Belcan  
2005-08 Biomedical Research Assistant – University of Kentucky  
2003-04 Mathematics Teacher – Saint James School

### Scholastic and Professional Honors

Golden Key Honor Society, Delta Epsilon Iota Academic Honor Society,  
Graduated Magna Cum Laude, Omicron Delta Kappa Leadership Honor Society,  
Sigma Gamma Tau Aerospace Engineering Honor Society

## Professional Publications (Abstracts)

**Howarth, Mark S.** Biomedical Research Model: What Can Be Applied to Development Engineering? *Lexmark Excellence Symposium Program (Abstract)*, 2011.

**Howarth MS,** Moore FB, Hinghofer-Szalkay H, Jezova D, Diedrich A, Ferris MB, Schlegel TT, Patwardhan AR, Knapp CF, and Evans JM. Exercise Increases the Cardiovascular Stimulus Provided by Artificial Gravity. *29<sup>th</sup> International Society for Gravitational Physiology Meeting Program (Abstract)*, 2008.

**Howarth MS,** Moore FB, Hinghofer-Szalkay H, Jezova D, Diedrich A, Ferris MB, Schlegel TT, Patwardhan AR, Knapp CF, and Evans JM. Thoracic impedance as a potential indicator of Gz-induced presyncope. *FASEB (Abstract)*, 2008.

**Howarth MS, et al.** Assessment of Countermeasures to Simulated Spaceflight Deconditioning: Recent Studies. *13<sup>th</sup> Annual Kentucky EPSCoR Conference Program (Abstract)*, 2007.

**Howarth MS,** Moore FB, Hinghofer-Szalkay H, Jantscher A, Stenger MB, Diedrich A, Patwardhan AR, Knapp CF, and Evans JM. Cardiovascular Responses to Artificial Gravity are Modulated by Radius of Rotation and Exercise. *FASEB (Abstract)*, 2007.

**Howarth MS,** Schlegel TT, Knapp CF, Patwardhan AR, Jenkins RA, Ilgner RH, and Evans JM. Cardiac Autonomic Effects of Acute Exposure to Airborne Particulates in Men and Women. *FASEB (Abstract)*, 2007.